

**THE IMPACT OF PROTECTIVE GROUNDING
DEVIATION ON THE SURGE PROTECTION
DEVICE**

H'NG SONG TIAN

UNIVERSITI TUNKU ABDUL RAHMAN

**THE IMPACT OF PROTECTIVE GROUNDING DEVIATION
ON THE SURGE PROTECTION DEVICE**

H'NG SONG TIAN


**A project report submitted in partial fulfilment of the
requirements for the award of Bachelor of Engineering
(Honours) Electrical and Electronic Engineering**

**Lee Kong Chian Faculty of Engineering and Science
Universiti Tunku Abdul Rahman**

April 2022

DECLARATION

I hereby declare that this project report is based on my original work except for citations and quotations which have been duly acknowledged. I also declare that it has not been previously and concurrently submitted for any other degree or award at UTAR or other institutions.

Signature : 

Name : H'NG SONG TIAN

ID No. : 1703593

Date : 15/5/2022

APPROVAL FOR SUBMISSION

I certify that this project report entitled “**THE IMPACT OF PROTECTIVE GROUNDING DEVIATION ON THE SURGE PROTECTION DEVICE**” was prepared by **H’NG SONG TIAN** has met the required standard for submission in partial fulfilment of the requirements for the award of Bachelor of Engineering (Honours) Electrical and Electronic Engineering at Universiti Tunku Abdul Rahman.

Approved by,

Signature

:



Supervisor

:

Dr. Chew Kuen Wao

Date

:

15/5/22

Signature

:

Co-Supervisor

:

Date

:

The copyright of this report belongs to the author under the terms of the copyright Act 1987 as qualified by Intellectual Property Policy of Universiti Tunku Abdul Rahman. Due acknowledgement shall always be made of the use of any material contained in, or derived from, this report.

© 2022, H'ng Song Tian. All right reserved.

ACKNOWLEDGEMENTS

I would like to thank everyone who had contributed to the successful completion of this project. I would like to express my gratitude to my research supervisor, Ts. Dr. Chew Kuew Wai for his invaluable advice, guidance and his enormous patience throughout the development of the research.

In addition, I would also like to express my gratitude to my loving parents and friends who had helped and given me encouragement to complete this project.

ABSTRACT

A power surge, such as lightning, destroys electrical and electronic components and threatens human life. Surge protection devices (SPD) are installed as a protective measure to prevent power surge events. However, the SPD requires good protective grounding to function well. Without adequate grounding, SPD may not be able to protect the system and the connected loads. This project investigates the effects of different earthing layouts, different grounding resistances, and the impact of harmonic distortion on SPD performance. The SPDs applied in this project are the conventional type (MOV) and the power device type (MOSFET). A surge generator that complies with the IEC 61000-4-5 standard is created and applied to these earthing layouts via MATLAB Simulink software. The SPD performance is not affected by the type of earthing layouts. The increase in grounding resistance value improves the clamping effect for the MOV but reduces for the MOSFET. Besides, when harmonic distortion is added, the protection efficiency for both SPDs is affected. Harmonic distortion affects the SPD performance by distorting the voltage supplied. The MOSFET has a better response time and fall time at lower grounding resistance than the MOV. However, when the grounding resistance increases, the MOV response time and fall time are faster. This shows that the MOSFET is suitable for earthing systems with low grounding resistance. In comparison, the MOV is suitable for the earthing system with high grounding resistance.

TABLE OF CONTENTS

DECLARATION		i
APPROVAL FOR SUBMISSION		ii
ACKNOWLEDGEMENTS		iv
ABSTRACT		v
TABLE OF CONTENTS		vi
LIST OF TABLES		ix
LIST OF FIGURES		x
LIST OF SYMBOLS / ABBREVIATIONS		xvi
LIST OF APPENDICES		xvii
CHAPTER		
1	INTRODUCTION	1
1.1	General Introduction	1
1.2	Importance of the Study	1
1.3	Problem Statement	2
1.4	Aim and Objectives	2
1.5	Scope and Limitation of the Study	2
1.6	Contribution of the Study	3
1.7	Outline of the Report	3
2	LITERATURE REVIEW	4
2.1	Introduction	4
2.2	Surge	4
2.2.1	External Source of Surge: Lightning	4
2.2.2	Internal Source of Surge	6
2.2.3	Generation of Surge Waveform	7
2.3	Surge Protection Device (SPD)	11
2.3.1	Operational Modes of SPD	11
2.3.2	Different Types of SPD	12
2.3.3	Protection Mode of SPD	14

	2.3.4 Components of SPD	15
	2.3.5 Power semiconductor device	19
2.4	Grounding System	20
	2.4.1 Types of Low Voltage Grounding System	20
	2.4.2 Grounding System Performance and Design	25
	2.4.3 Grounding Evaluation Methods	29
2.5	Harmonic	33
	2.5.1 Complex Waveform	33
	2.5.2 Harmonic Sequencing	34
	2.5.3 Impacts of Harmonic Distortion	35
3	METHODOLOGY AND WORK PLAN	36
	3.1 Introduction	36
	3.2 Surge/ Combination Waveform Generator Model	36
	3.3 Earthing System Network Model	37
	3.4 SPD	37
	3.5 Grounding Impedance Deviation	39
	3.6 Harmonic Distortion (Triplen Harmonic)	39
	3.7 Parameters to be study	40
	3.8 Workplan	40
4	RESULTS AND DISCUSSION	41
	4.1 Introduction	41
	4.2 Surge / Combination Wave Generator Model	41
	4.2.1 Derivation for Open Circuit Voltage formula	41
	4.2.2 Derivation for Short Circuit Current formula	42
	4.2.3 Derivation for parameter formula	43
	4.2.4 Results for circuit and waveform	45
	4.3 Different earthing system with surge applied	47
	4.4 MOV Performance	49
	4.4.1 Voltage clamped by MOV in different earthing system	50

4.4.2	Response Time and Fall Time of MOV in different earthing system	51
4.4.3	Impact of grounding resistance value on MOV performance	53
4.5	MOSFET Performance	55
4.5.1	MOSFET waveform during surge event	56
4.5.2	Response Time and Fall Time of MOSFET in different earthing system	60
4.5.3	Impact of grounding resistance value on MOSFET performance	62
4.6	Comparison between MOSFET and MOV performance	65
4.7	Harmonic distortion	66
4.7.1	Different earthing system with harmonic distortion applied	66
4.7.2	Effect of harmonic distortion on the MOV performance	68
4.7.3	Effect of harmonic distortion on the MOSFET performance	72
5	CONCLUSIONS AND RECOMMENDATIONS	76
5.1	Conclusions	76
5.2	Recommendations for future work	77
	REFERENCES	78
	APPENDICES	80

LIST OF TABLES

Table 2.1:	Classification of SPD defined by IEC and EN standards (LIGHTNING PROTECTION GUIDE 3rd updated Edition, 2015)	13
Table 2.2:	Multiplying factors for multiple electrodes	27
Table 2.3:	Multiplying factors for multiple electrodes (IEE 142, 2007)	28
Table 2.4:	Characteristics summary for grounding evaluation methods	29
Table 4.1:	Percentage error for the simulated open-circuit voltage waveform	45
Table 4.2:	Percentage error for the simulated open-circuit voltage waveform	47
Table 4.3:	Percentage error of the V_{rms} for the load	48
Table 4.4:	Summary of the MOV protection parameter in different grounding resistance	55
Table 4.5:	Summary of the MOSFET protection parameter in different grounding resistance	64
Table 4.6:	Comparison between the response time and fall time of the forward MOSFET and the MOV	66
Table 4.7:	Comparison of the MOV protection parameter between harmonic and normal condition	72
Table 4.8:	Comparison of the forward MOSFET protection parameter between harmonic and normal condition	76

LIST OF FIGURES

Figure 2.1:	Formation of thundercloud (Lightning & Surge Protection, 2021)	5
Figure 2.2:	Lightning production (Science Learning Hub, 2014)	5
Figure 2.3:	Graph of induced emf against the rate of change of current 7	7
Figure 2.4:	General surge waveform	7
Figure 2.5:	Surge waveform from double exponential shape (Klüss and Larzelere, 2017)	8
Figure 2.6:	1.2/50 μ s combination wave generator circuit (IEC 61000-4-5, 2014)	9
Figure 2.7:	1.2/50 μ s open circuit voltage waveform (IEC 61000-4-5, 2014)	9
Figure 2.8:	8/20 μ s short circuit current waveform (IEC 61000-4-5, 2014)	9
Figure 2.9:	10/700 μ s combination wave generator circuit (IEC 61000-4-5, 2014)	10
Figure 2.10:	10/700 μ s open circuit voltage waveform (IEC 61000-4-5, 2014)	10
Figure 2.11:	5/350 μ s short circuit current waveform (IEC 61000-4-5, 2014)	10
Figure 2.12:	Surge current flowing through SPD	12
Figure 2.13:	Installation examples for different class of SPD (IEC 60364-5-53, 2015)	12
Figure 2.14:	Type 1 SPD with impulse current rated at 25kA (ABB, n.d.)	13
Figure 2.15:	Type 2 SPD with maximum discharge current rated at 20kA (ABB, n.d.)	13
Figure 2.16:	Type 3 SPD with a maximum discharge current rated at 10kA (ABB, n.d.)	14
Figure 2.17:	Common mode protection	14

Figure 2.18:	Differential mode protection	15
Figure 2.19:	Internal components of SPD	15
Figure 2.20:	Metal oxide variastor (MOV)	16
Figure 2.21:	Overheat issue blows up the MOV)	16
Figure 2.22:	Gas discharge tube (GDT)	17
Figure 2.23:	Metal oxide variator resistance curve (electronicstutorials, n.d.)	18
Figure 2.24:	Metal oxide variator clamping performance	18
Figure 2.25:	Avalanche effect	19
Figure 2.26:	The characteristics for different power devices	20
Figure 2.27:	TT Grounding System	22
Figure 2.28:	IT Grounding System	23
Figure 2.29:	TN-C Grounding System	23
Figure 2.30:	TN-S Grounding System	24
Figure 2.31:	TN-C-S Grounding System)	25
Figure 2.32:	Effect of soil moisture content on soil resistivity (Mitolo, Sutherland and Natarajan, 2010)	26
Figure 2.33:	Two Point Method	30
Figure 2.34:	Three Point Method (Electrical Notes & Articles, 2020)	30
Figure 2.35:	The effects of distance on electrode resistance	31
Figure 2.36:	Four Point Method (Electrical Notes & Articles, 2020)	32
Figure 2.37:	Fundamental waveform (electronicstutorials, n.d.)	33
Figure 2.38:	Formation of complex waveform (electronicstutorials, n.d.)	33
Figure 2.39:	Rotating direction for the harmonic sequence	34
Figure 3.1:	1.2/50 μ s combine wave generator circuit	36
Figure 3.2:	Surge applied on the earthing system network models	37

Figure 3.3:	Connection of MOV in three earthing system network model	38
Figure 3.4:	Connection of MOSFET in three earthing system network model	38
Figure 3.5:	Simulation circuit for grounding impedance deviation at different earthing system with MOV connected	39
Figure 3.6:	Setting for triplen harmonic generation via three-phase AC source	40
Figure 3.7:	Experiment and simulation workplan	40
Figure 4.1:	IEC 61000-4-5 1.2/50 μ s open circuit voltage design	41
Figure 4.2:	IEC 61000-4-5 8/20 μ s short circuit voltage design	42
Figure 4.3:	Open-circuit voltage waveform with front time at 1.469 μ s	45
Figure 4.4:	Open-circuit voltage waveform with tail time at 50.327 μ s	45
Figure 4.5:	Short-circuit current waveform with undershoot peak value -196 A	46
Figure 4.6:	Short-circuit current surge waveform with front time at 7.653 μ s	46
Figure 4.7:	Short-circuit current surge waveform with tail time at 19.786 μ s	47
Figure 4.8:	Load voltage waveform in different earthing systems	48
Figure 4.9:	Load voltage waveform with surge in different earthing systems	49
Figure 4.10:	Overvoltage surge waveform in different earthing systems	49
Figure 4.11:	Load voltage waveform with MOV clamped surge in different earthing systems	50
Figure 4.12:	MOV clamped surge waveform in different earthing systems	51
Figure 4.13:	MOV clamped and unclamped surge waveform in TT earthing systems	51

Figure 4.14:	Measurement of the response time of MOV in TT earthing system	52
Figure 4.15:	Measurement of the fall time of MOV in TT earthing system	53
Figure 4.16:	Load voltage waveform with MOV when grounding resistance increases	54
Figure 4.17:	Load voltage waveform when grounding resistance increases	54
Figure 4.18:	MOV clamped waveform when grounding resistance increases	55
Figure 4.19:	MOV clamped waveform when grounding resistance increases	55
Figure 4.20:	Load voltage waveform with MOSFET in different earthing systems	56
Figure 4.21:	Load voltage waveform with MOSFET and surge in different earthing systems	57
Figure 4.22:	: Zoom in view of forward MOSFET switching transient waveform	58
Figure 4.23:	Operating current waveform of forward MOSFET with and without surge	59
Figure 4.24:	Zoom in view of forward MOSFET operating current waveform	59
Figure 4.25:	8/20 μ s short circuit current waveform (IEC 61000-4-5, 2014)	59
Figure 4.26:	Voltage of reverse MOSFET with and without surge	60
Figure 4.27:	Operating current waveform of reverse MOSFET with and without surge	60
Figure 4.28:	Forward MOSFET surge current waveform for different earthing system	61
Figure 4.29:	Measurement of the response time of forward MOSFET in TT earthing system	61
Figure 4.30:	Measurement of the fall time of forward MOSFET in TT earthing system	62

Figure 4.31:	Load voltage waveform with MOSFET when grounding resistance increases	62
Figure 4.32:	Operating current waveform of forward MOSFET when grounding resistance increases	63
Figure 4.33:	Surge current waveform of forward MOSFET when grounding resistance increases	63
Figure 4.34:	Surge current waveform of forward MOSFET when grounding resistance increases in TT earthing system	64
Figure 4.35:	Load voltage waveform with triplen harmonic in different earthing system	67
Figure 4.36:	Overvoltage surge waveform with triplen harmonic different earthing system	67
Figure 4.37:	Overvoltage surge waveform with triplen harmonic different earthing system	68
Figure 4.38:	Load voltage waveform with surge, harmonic and MOV applied in different earthing systems	69
Figure 4.39:	Load voltage waveform with and without harmonic at MOV TT earthing system	69
Figure 4.40:	Measurement of MOV response time with and without harmonic	70
Figure 4.41:	Measurement of MOV fall time with and without harmonic	70
Figure 4.42:	MOV clamped waveform at different earthing systems and grounding resistance with harmonic	71
Figure 4.43:	MOV clamped waveform at TT earthing systems and different grounding resistance with harmonic	71
Figure 4.44:	Forward MOSFET surge operating current waveform at different earthing system with harmonic applied	73
Figure 4.45:	Forward MOSFET surge operating current waveform at TT earthing system with and without harmonic applied	73
Figure 4.46:	Measurement of Forward MOSFET response time with and without harmonic applied	74
Figure 4.47:	Measurement of Forward MOSFET fall time with and without harmonic applied	74

- Figure 4.48: Forward MOSFET surge current waveform at different earthing systems and grounding resistance with harmonic 75
- Figure 4.49: Forward MOSFET surge current waveform at TT earthing systems and different grounding resistance with harmonic 75

LIST OF SYMBOLS / ABBREVIATIONS

a	gap between electrode in four-point method, m
D	earth electrode diameter, m
I_{ECA}	current flow between electrode E and probe C, A
L_e	earth electrode length, m
ρ	soil resistivity, Ωm
R_e	earth electrode resistance, Ω
R_g	grounding resistance, Ω
t_r	response time, μs
t_f	fall time, μs
$t_{0.5peak}$	time taken to reach half of the peak clamped value, μs
t_p	time taken to reach the peak clamped value, μs
t_s	start up time, μs
V_{p1p2}	potential difference between probe P ₁ and P ₂ , V
GDT	gas discharge tube
MOSFET	metal oxide semiconductor field effect transistor
MOV	metal oxide variastor
SPD	surge protection device

LIST OF APPENDICES

Appendix A: IEC 61000-4-5 STANDARD	80
------------------------------------	----

CHAPTER 1

INTRODUCTION

1.1 General Introduction

A surge protection device (SPD) is a device that protects the electrical network from any surge events. The SPD captures and channels the surge to the low resistance pathway in the grounding system of an electrical network. In electrical engineering, the term surge is a rapid burst of voltage energy. A surge event can be happened in an electrical network either from the outside or the inside. When an electrical network is affected by a surge, the electrical appliances connected within the electrical network will be damaged. As such, SPDs are installed in electrical networks. Since the surge is channelled to the earth, the deviation in the grounding system disturbs the functionality of the SPD. This project studies and investigate the effect of different grounding layout on the SPD protection efficiency.

1.2 Importance of the Study

Electricity plays an essential role in humankind's daily lives. However, the unpredictability nature of surge events damages sensitive electronics systems and electrical systems. If surge events are not correctly handled, such events will affect the daily activities in the urban and residential areas. Furthermore, the industrial sectors, such as medical, data, and production, would face operational failures and equipment and asset destruction. Notably, the financial losses due to unexpected downtime are considerably more significant than the value of the destroyed equipment. Thus, applying SPD in electrical networks is essential because it can prevent failures during surge events.

Although the SPD is a device that acts instantly upon the surge event, the SPD's functionality is somehow influenced by the connected grounding system. The grounding system impacts the SPD's functionality because every low voltage grounding system has its characteristics and working principles. Besides, the surrounding environment and the harmonic distortion in the grounding system also affect the functionality of the SPD. Thus, the effect of

different grounding layouts on the SPD protection efficiency and performance must be studied.

1.3 Problem Statement

Different SPDs were invented to serve as protection devices for grounding systems during a surge event. However, due to the mass usage of the digital signal in the current era, the failure of SPD to respond in the shortest time during surge event damage sensitive electronic device and electrical system. There is incompetency in the SPD because the installation of SPD on different grounding layouts did not consider the surrounding environment factor, the characteristics, and the impact of the harmonic distortion. Thus, it is vital to study and improve the performance of SPD on different grounding layouts.

1.4 Aim and Objectives

This project investigates the effect of different grounding layouts on SPD's protection efficiency. The focus of this project is:

- Perform studies on surge events and low voltage grounding systems.
- Investigate the SPD performance in different low voltage earthing layouts and grounding resistance.
- Study the impact of the harmonic distortion in the grounding on the SPD performance.

1.5 Scope and Limitation of the Study

Different low voltage grounding layouts are simulated with an indirect lightning surge. Each layout will contain a similar resistance load. Furthermore, different SPDs will be installed and simulated in each grounding layout. The generated surge waveform follows the 1.2/50 μ s double wave generator settings stated in the IEC 61000-4-5 standard. This project will not simulate the direct lightning strike event due to the waveform of 100/350 μ s which is very high and hard to control.

As the university is locked down during the pandemic, this project cannot do hardware simulation without access to the laboratory. Since all experimental results are obtained from software simulation, environmental

factors such as the soil mineral content, moisture content, and soil resistivity that affect the grounding system performance are all neglected.

1.6 Contribution of the Study

This project is a necessary research and development that contributes to the electrical protection field. By studying and investigating the SPD in different earthing layouts and grounding resistance, this project can further verify the reliability and characteristics of the SPD. Besides, this project can also verify the weakness and shortcomings of the SPD operating under harmonic conditions. This investigation will eventually allow improvements and new technologies to be developed. As such, the harmful effects of the surge event can be further prevented and handled in a safer method.

1.7 Outline of the Report

There are five chapters in this finalized report. This section will give a rough explanation of the overall contents of each chapter.

The first chapter focuses on introducing the project title. Information such as the purpose, objectives, importance, contribution, limitation, and scope of this project is explained in this chapter. The second chapter provides a summary of the reviewed information and the findings related to this project. Besides, important source such as journals and research papers has contributed a lot to the reviews in this chapter.

The third chapter explains the steps, components, and parameters needed to carry out the simulation and study for the project. All the circuit layouts applied in the experiment are provided in this section. The fourth chapter displays and discusses the result obtained from the experiment. Results such as the clamping waveform and the SPD response time data are included in this chapter. The final chapter summarizes the project's findings and provides recommendations for future works.

CHAPTER 2

LITERATURE REVIEW

2.1 Introduction

This literature review contains three important topics. In the first topic, the theory and characteristics of the surge are studied. Next, the types and functionality of the SPD are also reviewed. Thirdly, different grounding layouts and the grounding factors that affect the SPD's performance are reviewed. Lastly, harmonic sequencing and the effects of harmonic distortion are also explored.

2.2 Surge

A surge is an unexpected and short event that increases the voltage level rapidly in an electrical system. This event usually occurs between microseconds to a few milliseconds and may happen externally or internally in an electrical system. According to the National Electrical Manufacturers Association (NEMA) (March, 2018), about 80% of the surge events are created inside a facility. At the same time, the surge events due to external sources hold a 20% probability. The surge can lead to many unwanted consequences such as facilities destruction and human death. Thus, SPD must be installed as a safety measure.

2.2.1 External Source of Surge: Lightning

Any surge event outside of an electrical system or facility is known as an external surge source. Examples of surges from an external source are lightning strikes, switching a utilities' capacitor bank, and power quality disturbance.

Lightning strikes are the most typical external source of surge. It happens when negative electric charges produced in a thunderstorm discharge to the ground, causing dielectric breakdowns in the air. The thunderstorms are formed due to the thunderclouds. Due to the evaporation process on the Earth's surface, all water vapours will transform into a cloud that contains water droplets in the atmosphere. As the cloud in the atmosphere rises higher, the water droplets within the cloud become concentrated and solidify into ice grains

and hailstones. At the same time, these substances are induced by electric current, causing each to contain a charge with different polarity. (Lightning & Surge Protection, 2021) Figure 2.1 illustrates the thundercloud formation.

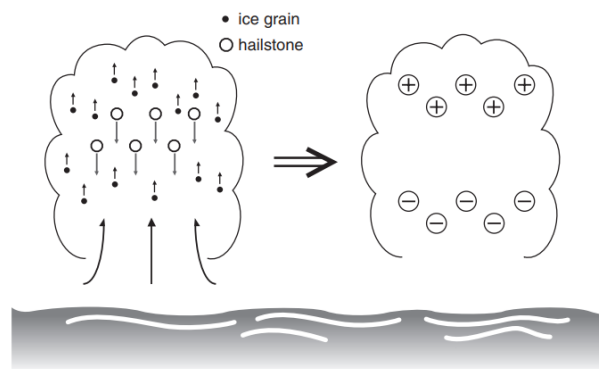


Figure 2.1: Formation of thundercloud (Lightning & Surge Protection, 2021)

All ice grains that are positively charged accumulate at the cloud's upper section due to updraft riding. In contrast, all negatively charged hailstones got more significant in size and gravitated to the bottom section of the cloud. The Coulomb force also affects the separation process of ice grains and hailstones according to charge. As such, electrical energy is stored within the cloud, causing thunderclouds to be formed.

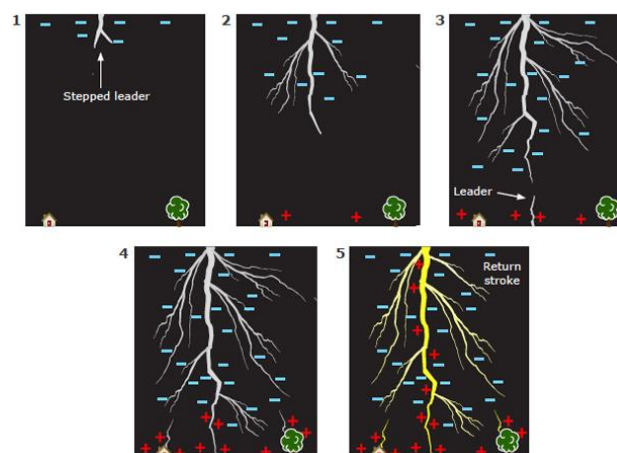


Figure 2.2: Lightning production (Science Learning Hub, 2014)

The movement and exchange of charge cause the lightning strike. The formation of thunderclouds induced a positively charged field on the ground. This field creates a potential difference between the space of the thundercloud

and the ground. (Science Learning Hub, 2014) When the voltage reaches a particular level, electrical conductivity is formed between this space. Next, a stepped leader is created during the first lightning discharge. The stepped leader streams from the thundercloud to connect with the ground's leader. This connection establishes a channel between the thundercloud and the ground, allowing positive ions and electrons to exchange. Thus, a lightning strike is formed when charges flow between the thundercloud and the ground. The lightning production is shown in Figure 2.2.

2.2.2 Internal Source of Surge

A surge event that arises from any factors inside an electrical system is classified as an internal surge. Examples of internal surge sources are switching on and off electrical load, magnetic and inductive coupling, and static electricity. Since there are always many capacitive and inductive loads connected to an electrical system, load switching contributes the most to the internal surge events. The resistive load within the electrical system will not cause any surge event because there is no current left when power is switched off.

2.2.2.1 Switching of Inductive Load

The inductive load is a device that performs mechanical work with a magnetic coil. A magnetic field is formed around the coil when the current passes through it. Although no current will be supplied when the inductive load is switched off immediately, the vanished magnetic field produces current flowing back to the power source. This backflow current produces an induced e.m.f that is much more significant and destructive than the supplied voltage. The high induced e.m.f is influenced by the load inductance and the rate of change of current. The faster the change in current, the greater the induced e.m.f produced. Figure 2.3 shows a graph for the induced e.m.f. against the current change rate. The induced emf increases negatively due to the backflow current. Thus, a switching surge happens because the quick-change rate of current creates a destructive induced e.m.f. Example of inductive loads is motor, transformer, and power generators.

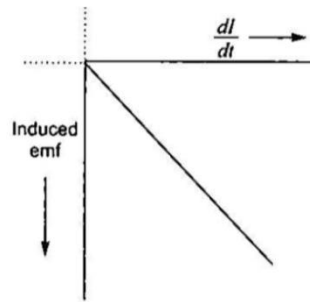


Figure 2.3: Graph of induced emf against the rate of change of current

2.2.2.2 Switching of Capacitive Load

The capacitive load is a device that contains capacitance to store electrical charges. Due to the capacitive load's nature that resists changes in voltage, the current will always reach the 90° peak phase before the voltage in each electrical cycle. The capacitive load is a power factor improvement device to solve the lagging power issue. When a capacitive load is switched on, many currents rush into the capacitor for charging. As the inrush current is more significant than the relay contacts' steady-state current, capacitive load switching produces a switching surge.

2.2.3 Generation of Surge Waveform

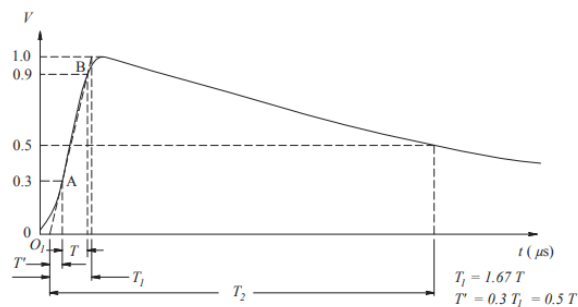


Figure 2.4: General surge waveform

Figure 2.4 shows the general surge waveform. Due to the surge event that causes a sudden rise in voltage, the waveform increases quickly to the peak and declines slowly to zero value. The equation below represents the function of the surge waveform:

$$v(t) = V(e^{-\alpha t} - e^{-\beta t}) \quad (2.1)$$

Where α and β represent constant with microseconds as a unit. The surge waveform is a unidirectional impulse that contains a double exponential shape, as depicted in Figure 2.5. This double exponential shape is equivalent to the difference of two exponentially decaying waveforms of identical amplitude.

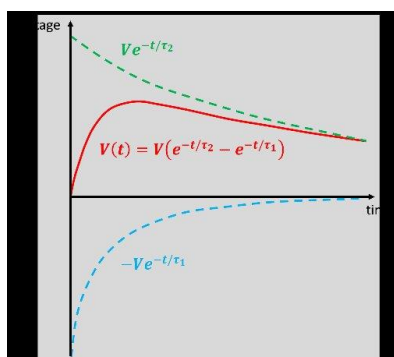


Figure 2.5: Surge waveform from double exponential shape (Klüss and Larzelere, 2017)

The two essential characteristics of surge waveform are the front time, T_f and the tail time, T_t . The T_f is the duration for the waveform to achieve the peak value. In comparison, the T_t is the duration to decline from the waveform's peak value to half of the peak value. Since surge is created from different sources, the surge waveform produced will also vary. However, to allow simulation and testing purposes, this surge waveform must be reproduced.

A combination generator circuit that produces a surge in a voltage waveform and a current waveform is invented. The produced waveform is defined via the T_f and T_t . The IEC 6100-4-5 Standard provides two combination wave generators classified as 1.2/50 μs and 10/700 μs .

Figure 2.6 shows the 1.2/50 μs combination wave generator circuit that produces a 1.2/50 μs voltage waveform under open-circuit conditions. When the generator is short-circuited, an 8/20 μs current waveform is produced. The waveform produced by this generator represents the surge event due to indirect lightning strikes. According to the IEC 6100-4-5 Standards guideline, the effective output impedance of the combination wave generator is defined as the ratio between the maximum open-circuit voltage and the peak short-circuit current. The effective output impedance for this generator is 2 Ω . Figure 2.7 and

2.8 shows the open-circuit voltage waveform and short-circuit current waveform of the 1.2/50 μs combination wave generator circuit defined by the IEC 61000-4-5 standard.

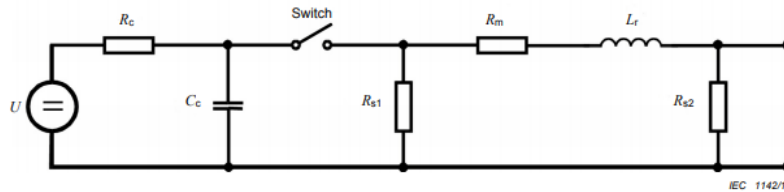


Figure 2.6: 1.2/50 μs combination wave generator circuit (IEC 61000-4-5, 2014)

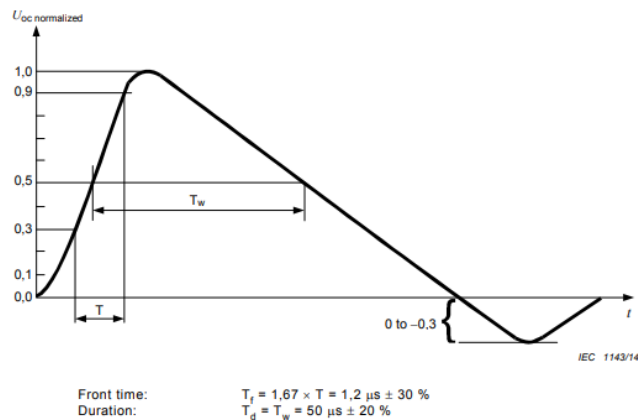


Figure 2.7: 1.2/50 μs open circuit voltage waveform (IEC 61000-4-5, 2014)

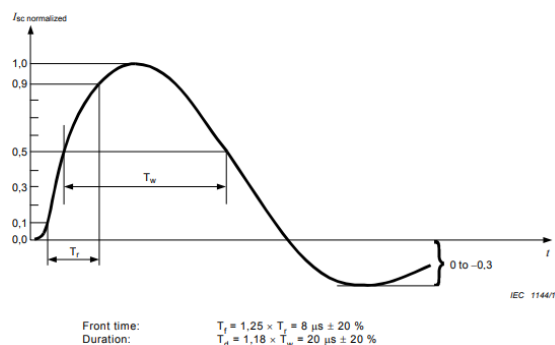


Figure 2.8: 8/20 μs short circuit current waveform (IEC 61000-4-5, 2014)

Figure 2.9 shows the 10/700 μs combination wave generator circuit that produces a 10/700 μs voltage waveform under open-circuit conditions. When the generator is short-circuited, a 5/350 μs current waveform is produced. The waveform produced by this generator represents the surge event due to direct

lightning strikes. The effective output impedance for this generator is 40Ω . Figure 2.10 and 2.11 shows the open-circuit voltage waveform and short-circuit current waveform of the 10/700 μs combination wave generator circuit defined by the IEC 61000-4-5 standard.

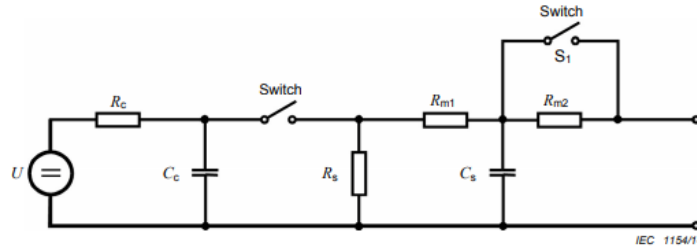


Figure 2.9: 10/700 μs combination wave generator circuit (IEC 61000-4-5, 2014)

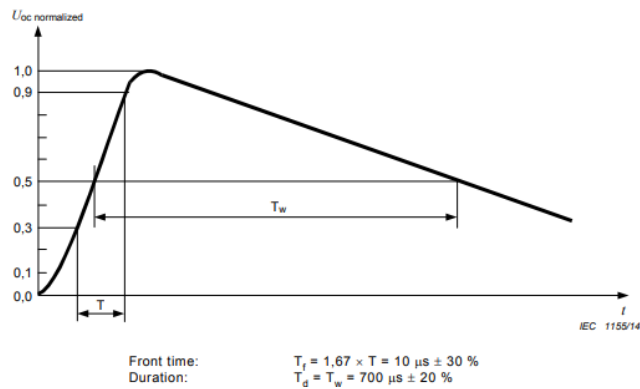


Figure 2.10: 10/700 μs open circuit voltage waveform (IEC 61000-4-5, 2014)

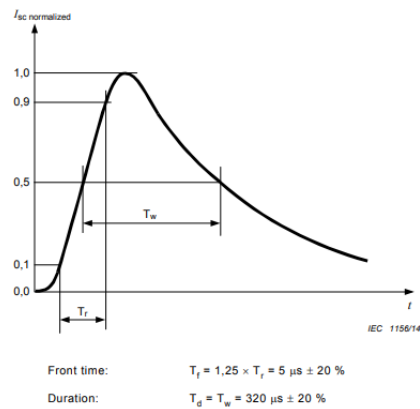


Figure 2.11: 5/350 μs short circuit current waveform (IEC 61000-4-5, 2014)

2.3 Surge Protection Device (SPD)

The surge protection device (SPD) is designed to safeguard the electrical system and loads from surge current, and overvoltage produced by lightning and electric switching. The SPD primary function is to create a low impedance pathway that diverts the surge to the ground, isolating and protecting the downstream equipment during a surge event. The main components inside the SPD are the metal oxide varistor (MOV) and gas discharge tube (GDT).

2.3.1 Operational Modes of SPD

The SPD contains two operating modes, the idle mode and the diverting mode. The SPD in the idle mode contains high impedance and operates under normal voltage conditions. In this mode, the SPD consumes very little power and waits for a surge event to occur. Currents can flow through the SPD and are supplied to the downstream equipment.

Normally, SPD will be installed parallel against the load that needs surge protection. When a surge event occurs, the SPD will change into diverting mode and decreases the SPD's impedance level. The sudden change of SPD to low impedance creates a low impedance pathway to the ground. The surge current will be diverted to the ground through this pathway and all downstream equipment's are protected from the surge event. When the current level across the SPD decreases, the impedance level of the SPD rises again. As such, the current supply for the downstream equipment is restored again. Figure 2.12 illustrates the surge current flowing through the SPD. The working principle of the SPD are summarized as below:

1. Maintain high impedance level and ensure current supply for downstream equipment during normal voltage condition.
2. Decrease impedance level to create low resistance pathway and divert surge to ground during surge events.
3. Restore high impedance level after channelling surge currents to ground.

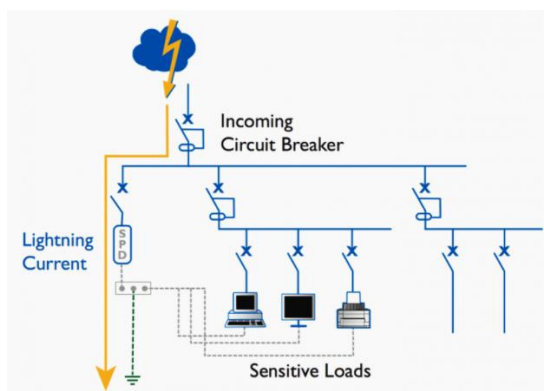


Figure 2.12: Surge current flowing through SPD

2.3.2 Different Types of SPD

Based on the IEC 61643-11 standards and EN 61634-11 standards, the SPD can be classified into three different types. The SPD classification is defined according to the surge source. Table 2.1 shows the summary for different types of SPD. Figure 2.13 shows the suggested installation location by the IEC 60634-5-53 standards.

Table 2.1: Classification of SPD defined by IEC and EN standards (LIGHTNING PROTECTION GUIDE 3rd updated Edition, 2015)

Type / designation	Standard	EN 61643-11:2012	IEC 61643-11:2011
Lightning current arrester / combined arrester		Type 1 SPD	Class I SPD
Surge arrester for distribution boards, sub-distribution boards, fixed installations		Type 2 SPD	Class II SPD
Surge arrester for socket outlets / terminal devices		Type 3 SPD	Class III SPD

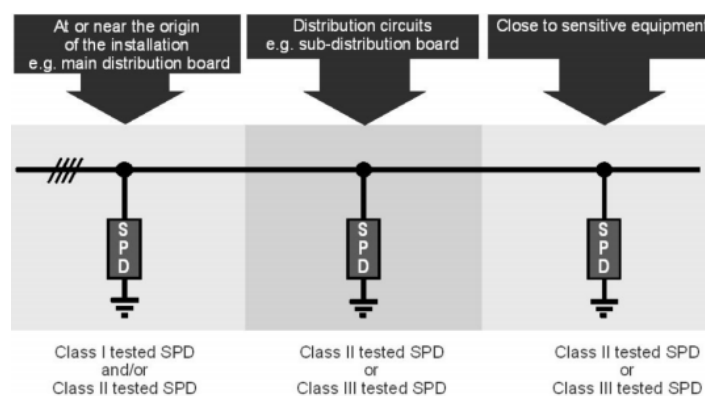


Figure 2.13: Installation examples for different class of SPD (IEC 60364-5-53, 2015)

The Type 1 SPD is characterized by 10/350 μ s current waveform. It is the highest class among the SPD type because it discharges the highest current waveform produced by direct lightning strikes. The Type 1 SPD is generally installed before the main circuit breaker in the main distribution box. Figure 2.14 shows a lightning current arrester of the Type 1 SPD with an impulse current rated at 25kA.

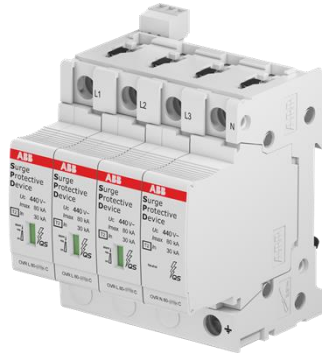


Figure 2.14: Type 1 SPD with impulse current rated at 25kA (ABB, n.d.)

The Type 2 SPD is characterized by 8/20 μ s current waveform. It discharges the current waveform produced by indirect lightning strikes and switching surges. This SPD usually serves as a protection for low voltage electrical systems. They are usually applied at the sub-distribution box or main distribution box in a residential area. Figure 2.15 shows a surge arrester of the Type 2 SPD with maximum discharge current rated at 20kA.



Figure 2.15: Type 2 SPD with maximum discharge current rated at 20kA (ABB, n.d.)

The Type 3 SPD has a combination characteristics of 8/20 μ s current waveform and 1.2/50 μ s voltage waveform. It discharges the surge produced between conductors in an electrical system, which is the home appliances. This SPD acts as an additional protection device after the Type 2 SPD and is usually installed before the circuit breaker of electrical load at the sub-distribution box. Figure 2.16 shows a surge arrester of the Type 3 SPD with a maximum discharge current rated at 10kA.



Figure 2.16: Type 3 SPD with a maximum discharge current rated at 10kA (ABB, n.d.)

2.3.3 Protection Mode of SPD

The common mode and the differential mode are the two protection modes in SPD. According to the IEC 60634-5-53 standard, common mode protection is formed when the SPD is installed between live conductors and potential earth (PE). There is common mode protection because this mode protects earthed equipment from the surge between the live conductors and the ground. Figure 2.17 illustrates the common mode protection of an SPD.

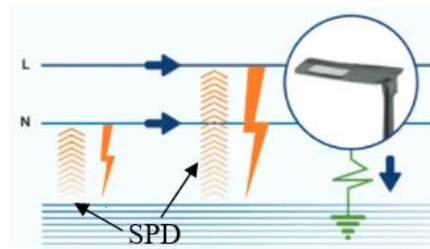


Figure 2.17: Common mode protection

If the SPD is installed between phase-to-phase or phase-to-neutral, a differential mode protection is formed. The differential mode protects the

connected equipment from overvoltage that happens between the phase and neutral conductors. The differential mode protection is essential because such overvoltage may destroy all the equipment connected to the electrical system. The common mode diverts the surge to the ground only. In comparison, the differential mode diverts the surge to the ground or other live conductors. Figure 2.18 illustrates the differential mode protection of an SPD.

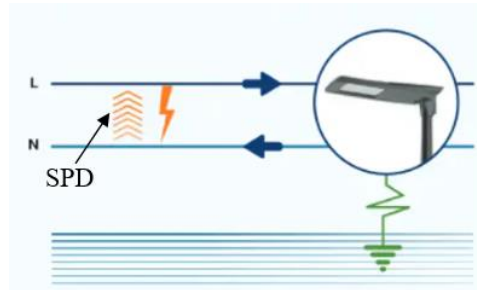


Figure 2.18: Differential mode protection

2.3.4 Components of SPD

The SPD is made up of four components, just as depicted in Figure 2.19. The first component is a non-linear component. The non-linear components are the main component, and there is usually one or more in an SPD. Examples of the non-linear components are metal oxide varistor (MOV) and gas discharge tubes (GDT). The second component is the thermal protective device which will disconnect upon a thermal runaway at the varistor. The third component is a lifespan indicator. The last component is an internal short circuit protection device (SCPD) that protects the SPD from short circuit events.

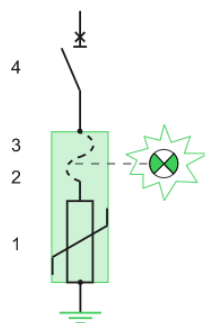


Figure 2.19: Internal components of SPD

2.3.4.1 Device Type for Non-linear component

The non-linear components contain two device types: clamping device and crowbar device. The clamping device allows consumer load to stay operated during a surge event. This is because the device only clamps off the voltage level above the device's voltage limit and allows a steady current to be supplied to the load. This causes the clamped voltage to be separated from the load and channels the extra current to the ground, ensuring the load still receives sufficient current for operating. The extra current is channelled to the ground because the clamping device's internal impedance changes from high to low when the SPD detects a surge. Examples of clamping devices are the metal oxide varistor (MOV) and Zener diode. Figure 2.20 shows the image of a metal oxide variator (MOV).



Figure 2.20: Metal oxide variastor (MOV)

The clamping device usually encounters overheating issues when diverting the surge current. Since the internal impedance of the clamping device is reduced from high to low, the low-level internal impedance in the device will cause a heating issue when the high-level surge current passes through the device. The clamping device will be significantly damaged when operating under an overheat situation for too long. This situation is shown in Figure 2.21. Anyway, the clamping device has a better performance than the crowbar device due to the faster response time.



Figure 2.21: Overheat issue blows up the MOV

Unlike the clamping device, the load connected will stop operating when the crowbar device starts the protection mechanism. The crowbar device controls the conductive gases contained within the device. This device applies the crowbar's methodology in a circuit breaker that trips by releasing the crowbar metal bit during a fault event. Similarly, due to the high impulse voltage, the conductive gases in the device undergo the ionization and breakdown process. This process is known as the avalanche effect, establishing a short circuit path to the ground. There will be lesser insulation in the device when the number of conductive gases increases. This condition allows the channelling of the surge current via the low impedance path. An example of the clamping device type SPD is the gas discharge tube (GDT) which is shown in Figure 2.22



Figure 2.22: Gas discharge tube (GDT)

The disadvantage of the crowbar device is no power will be supplied to the load when the device operates. When a short circuit path to the ground is established via the crowbar device, the supply current and the surge current are diverted to the ground instead of the load. Thus, the load will not maintain its operating mode as no current is supplied. Due to this reason, the crowbar device is not equipped with the load in important sectors such as medical facilities and the manufacturing industry. Secondly, the response time of a crowbar device is slower because time is needed for the ionization and breakdown process of the conduction gas.

2.3.4.2 Metal Oxide Variator (MOV)

One well-known clamping device is the metal oxide varistor (MOV). The MOV comprises two metal plates enclosed with many kinds of metal oxides and zinc oxides. These enclosed oxides act as the resistive components in the MOV, and the resistance is infinite. Due to this, the MOV is very sensitive to the transient

voltage, and they absorb when the voltage limit is exceeded. As such, the voltage across the MOV controls the internal resistance level. As shown in the resistance curve in Figure 2.23, the resistance level of the MOV decreases nearly to zero when the voltage level increases rapidly.

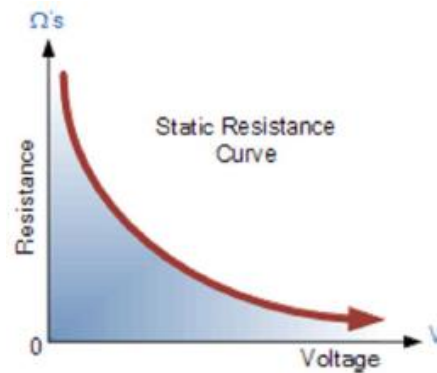


Figure 2.23: Metal oxide variator resistance curve (electronicstutorials, n.d.)

When the MOV operates under normal voltage conditions, the MOV does not consume much power and acts in idle mode. Once there is voltage spike, the high internal resistance of the MOV is induced and reduced to a low level. The MOV is chosen as a protection device for the surge event with this ability. This is because the surge current will be diverted to the ground when the internal resistance is low. Figure 2.24 shows the clamping performance of the MOV on the voltage spike waveform.

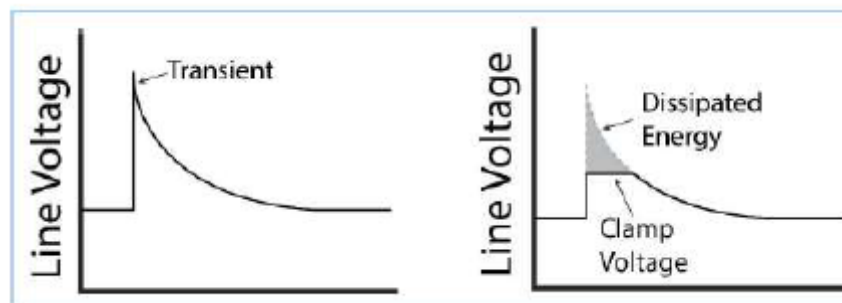


Figure 2.24: Metal oxide variator clamping performance

2.3.4.3 Gas Discharged Tube (GDT)

The gas discharge tube (GDT) is categorized as a crowbar device type SPD. It comprises two electrodes enclosed with ionizable gas such as hydrogen,

deuterium, noble, etc. The container of the GDT is mainly made up of ceramics. The GDT functions like a voltage-dependent switch, having a high impedance level to remain at the off state. When the GDT encounters the voltage spike by the surge event, the ionization process occurs on the enclosed gas, creating free electrons. These free electrons will move towards the positive terminal of the GDT. A collision happens between the free electron and the gas particles when moving. As such, more gas particles undergo the ionization process. This situation is shown in Figure 2.25 and is known as the avalanche effect. When the gas particles inside the GDT are completely ionized, the two electrodes will be connected. Thus, the GDT creates a short circuit path to the ground, diverting the surge current during a surge event.

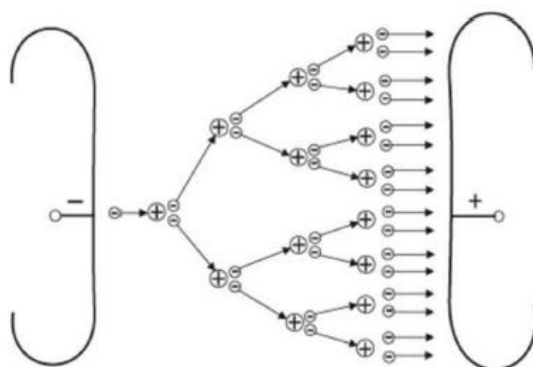


Figure 2.25: Avalanche effect

2.3.5 Power semiconductor device

A power semiconductor device, also known as a power device, is a power electronic that functions as a switch or a rectifier. Different kinds of power devices are developed so that the device's operation frequency and power capability are improved. Examples of power devices are the MOSFET, thyristor, IGBT, and GTO. Figure 2.26 depicts the operation frequency and power capability of different power devices. As shown in Figure 2.26, the MOSFET has the fastest operation frequency, whereas the thyristor has the most significant power capability. The MOSFET that has the fastest operation frequency also means that it has the fastest response time.

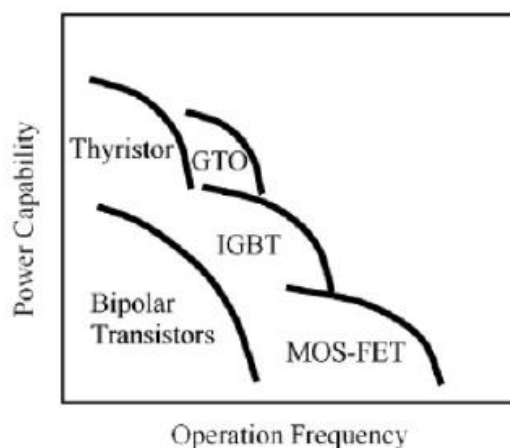


Figure 2.26: The characteristics for different power devices

A power device such as the MOSFET might be a new type of SPD. This is because by using the fast-switching ability of the MOSFET, the MOSFET might replace the crowbar device that has a prolonged response time. Besides, the activated MOSFET can also establish a short circuit path similar to the crowbar device. When activated, the source terminal and drain terminal of MOSFET will be connected. This condition will allow a MOSFET connecting to the ground to divert the surge current. Thus, the power device such as the MOSFET might be a new replacement for the crowbar device such as the GDT.

2.4 Grounding System

A grounding system or an earthing system is a protective electrical system that aims in discharging electrical fault or surge via a low impedance path to the earth. The grounding system is formed by connecting the electrical system with the ground. The term “earthing” and “grounding” both carries the same meaning. However, different countries and different standards practice the terms differently. The term “earthing” is more commonly practised in Britain, Europe, and most commonwealth countries standards (IEC, IS). The term “grounding” is more applied among the North American standards (NEC, IEEE, ANSI, UL).

2.4.1 Types of Low Voltage Grounding System

The IEC 60364-4-41 is a standard that provides guidelines about the protection methods, including protective conductors for indirect contacts fault events. According to this standard, the grounding system for a low voltage distribution

system contains two different grounding's locations. The first grounding location is at the low voltage side of the supplier's distribution transformer. The second grounding is applied at the consumer's electrical installations. All grounding points are installed with a low impedance electrode. There are five grounding systems defined by this standard: TT system, TN-C system, TN-S system, TN-C-S system and IT system.

The letter's position illustrates the grounding characteristics of the grounding system. The grounding condition at the supplier side is described in the first letter, where:

- "T" indicates a direct grounding is made from the distribution transformer's neutral point to the earth. "T" is derived from the term "Terra" of ancient Greek, which means earth.
- "I" stands for isolated, meaning the transformer at the supplier side is not grounded or is grounded via a high impedance.

The second letter describes the grounding conditions of the electrical installations at the consumer side:

- "T" indicates the electrical installation is grounded directly.
- "N" indicates the electrical installation is connected to the transformer's grounding point of the supplier side through a neutral conductor.

The following letters describe the connection patterns between the neutral and the protective conductor:

- "C" stands for combined, meaning that the neutral conductor and protective conductor are merged (PEN conductor).
- "S" stands for separated, meaning that the neutral conductor and protective conductor are connected separately.

2.4.1.1 TT Grounding System

The TT grounding system has two grounding points, one located at the source side and the other located at the consumer side. In the TT system, the distributor will only provide grounding for the source. The consumer is responsible for providing their grounding point, which may be accomplished by placing a suitable ground electrode near the installation. The TT system is the grounding

system commonly applied in Malaysia. The locations and facilities suitable for the TT system are housing areas, locations with overhead distribution, telecommunication sites and agricultural areas. The TT system is suitable for telecommunication sites because this system reduces the conducted interference and noise appeared. Besides, when the overhead distribution is connected with fallen trees or branches, the earth conductor remains grounded and will not turn into live. Figure 2.27 illustrates the connection layout of the TT grounding system.

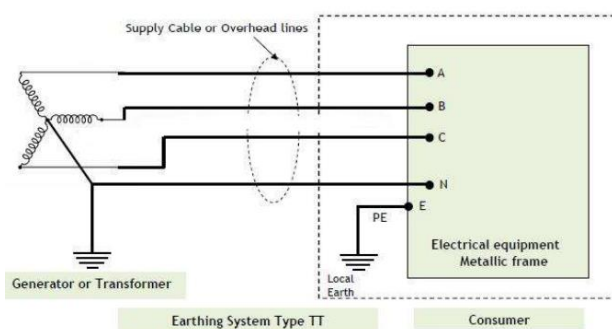


Figure 2.27: TT Grounding System

2.4.1.2 IT Grounding System

The IT grounding system contains two remote grounding points. The grounding point at the source side is defined as isolated because a high impedance separates the transformer's neutral point and the ground. The main advantage of this system is its ability to secure the continuous operation of other loads even if a load is affected by a fault event. When a first fault happens, the circuit breakers in the electrical system will remain inactivated because the fault current is diverted to the earth. This first fault will only be detected via a LED alarm, which helps locate the fault location during maintenance service. If a second fault happens before the first fault is cleared, this fault will short-circuit the whole electrical system, and the circuit breakers will be triggered. A monitoring device such as the LED alarm is applied to allow the first fault to be cleared quickly before the second fault happens. Due to the continuous operation ability during fault events, the IT system is usually applied to facilities that cannot afford power outages. Examples are hospitals, military defensive facilities and

data centres. Figure 2.28 illustrates the connection layout of the IT grounding system.

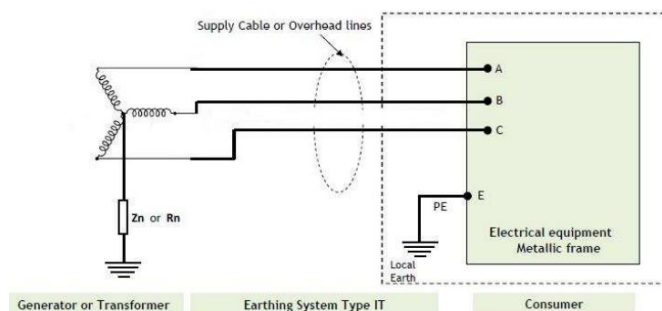


Figure 2.28: IT Grounding System

2.4.1.3 TN-C Grounding System

The TN-C grounding system includes a grounding point at the source side and a combined neutral protective (PEN) conductor. Similar to the other system, the source grounding point is connected with the transformer's neutral point. The PEN conductor is connected between the supplier's transformer neutral points and the consumer's electrical installation earth side. In the PEN conductor, the protective conductor function is more superior to the neutral conductor. The fault current at the load side is diverted to the PEN conductor back to the source grounding point during fault events. The TN-C system is applied at areas where all customers are interconnected and with a low voltage grid. The location examples are shopping malls, shop lots and housing areas. Figure 2.29 illustrates the connection layout of the TN-C grounding system.

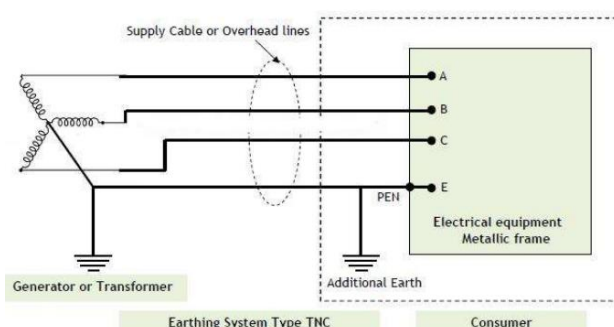


Figure 2.29: TN-C Grounding System

2.4.1.4 TN-S Grounding System

For the TN-S grounding system, a grounding point with a low impedance electrode is applied at the source. Besides, the neutral conductor (N) and the protective conductor (PE) in this system are separated. The N conductor is connected to the neutral side for both the source's transformer and the consumer's electrical installation. At the same time, the PE conductor is connected to the neutral side of the source's transformer and the earth side of the consumer's electrical installation. The fault current can flow through either the PE conductor or N conductor back to the source grounding point during a fault event. The TN-S system is suitable to apply for underground power supplies, large consumers with one or more step down transformers and locations with loads above 1 MA. Figure 2.30 illustrates the connection layout of the TN-S grounding system.

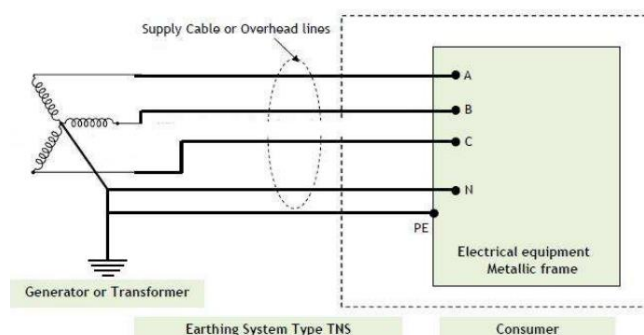


Figure 2.30: TN-S Grounding System

2.4.1.5 TN-C-S Grounding System

In the TN-C-S grounding system, the source's transformer is grounded with a low impedance electrode. Similar to the TN-C system, the TN-C-S system applies a PEN conductor which is connected to the source's transformer neutral point. The PEN conductor remains unseparated if there is no connection required to be established at the consumer side. When connecting to the consumer's electrical installation, the PEN conductor is separated into PE conductor and N conductor. The PE conductor will be connected to the electrical installation earth side and the N conductor will be connected to the neutral point. The TN-C-S system is usually applied at area with electromagnetic compatibility problems, such as radio tower and cell tower. Besides, this system

is also applied at the operators' distribution network. This is because the PEN conductor reduces the voltage drop during transmission and also reduces cabling cost. Figure 2.31 illustrates the connection layout of the TNC-S grounding system.

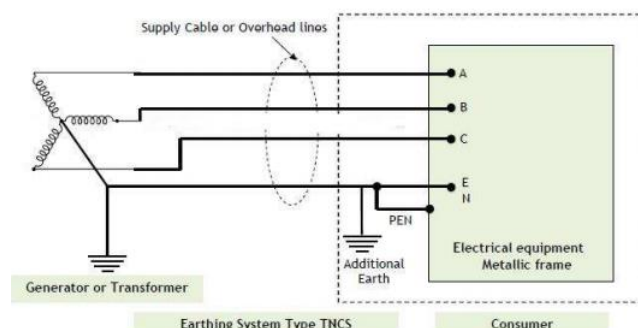


Figure 2.31: TN-C-S Grounding System

2.4.2 Grounding System Performance and Design

The criteria that must be taken care of when installing the grounding system are discussed in this section. The criteria are soil resistivity, factors affecting soil resistivity and the resistance of earth electrode.

2.4.2.1 Soil Resistivity

All electrical faults will be diverted to the ground because the ground contains unlimited positive charges to receive substantial currents. However, the high soil resistivity impacts the grounding system performance by preventing the fault current from discharging to the ground. The soil resistivity is affected by three factors: moisture contents, mineral content, and soil type.

Figure 2.32 shows the relationship between the soil resistivity against the moisture content for different types of soil. Based on this figure, the soil resistivity decreases when the soil moisture content increases. The soil moisture content is measured as a percent by weight. A soil with high moisture content contains many water particles. These water particles reduce the soil resistivity by filling up the pore spaces in the soil. (Kazmi et al., 2016) As such, the soil resistivity decreases, allowing the discharge of fault current to the ground. Earth electrodes are usually installed deeply in the ground to ensure that the soil's

moisture content is constant. If installed near the ground surface, environmental factors such as the drought and rainy season will affect the soil moisture content.

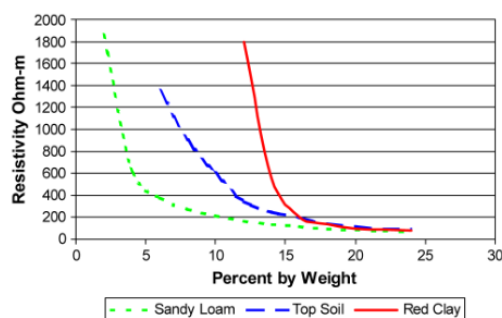


Figure 2.32: Effect of soil moisture content on soil resistivity (Mitolo, Sutherland and Natarajan, 2010)

The effect of mineral content on the soil resistivity is more superior to the soil moisture content. A soil with high mineral content will have low resistivity. This is because mineral content combines with the moisture content in the soil to produce electrolyte that allows current conduction. (Mari, 2020) Artificial mineral contents are usually added to the soil for soil resistivity enhancement. The artificial mineral examples are calcium, nitrates, chlorides, and magnesium. Although adding the artificial mineral to the ground reduces soil resistivity quickly, soil corrosion issues may happen. Hence, careful investigation and studies on the soil nature must be carried out before adding any artificial mineral.

The soil type also affects the soil resistivity because different type of soil has different compactness level. A least compact soil has a high soil resistivity. For instance, a rocky terrain that contains many air gaps between the rock arrangement will have high soil resistivity. Soil with high compactness will have low soil resistivity because the closely packed soil's particles allow the formed electrolyte to interact and conduct electricity. Thus, the soil resistivity decreases as the soil compactness increase.

2.4.2.2 Resistance of Earth Electrode

It is essential to select a suitable earth electrode resistance in the grounding system according to the soil resistivity. The discharging of fault current to the ground may fail if the earth electrode resistance cannot offset the high soil

resistivity. According to BS 7430 earthing installation codes, the earth electrode resistance can be calculated via the equation:

$$R_e = \frac{\rho}{2\pi L_e} \left[\log_e \left(\frac{8L_e}{d} \right) - 1 \right] \quad (2.2)$$

Where:

R_e = earth electrode resistance, Ω

ρ = soil resistivity, Ωm

L_e = earth electrode length, m

d = earth electrode diameter, m

In contrast, the IEEE 142 stated that the electrodes applied usually contain a length of 3 m and a diameter of 16 mm. Thus, based on these electrode settings, the simplified equation is:

$$R_e = \frac{\rho}{298} \quad (2.3)$$

Where:

R_e = earth electrode resistance, Ω

ρ = soil resistivity, Ωcm

In Table 2.2, the IEE 142 standard summarizes the recommended earth electrode resistance for different types of soil resistivity.

Table 2.2: Multiplying factors for multiple electrodes

Soil description	Group symbol ^a	Average resistivity (ohm-cm)	Resistance of 15.88 mm x 3 m (5/8 in x 10 ft) rod (ohm)
Well-graded gravel, gravel-sand mixtures, little or no fines	GW	60 000 to 100 000	180 to 300
Poorly graded gravels, gravel-sand mixtures, little or no fines	GP	100 000 to 250 000	300 to 750
Clayey gravel, poorly graded gravel, sand-clay mixtures	GC	20 000 to 40 000	60 to 120
Silty sands, poorly graded sand-silts mixtures	SM	10 000 to 50 000	30 to 150
Clayey sands, poorly graded sand-clay mixtures	SC	5000 to 20 000	15 to 60
Silty or clayey fine sands with slight plasticity	ML	3000 to 8000	9 to 24
Fine sandy or silty soils, elastic silts	MH	8000 to 30 000	24 to 90
Gravelly clays, sandy clays, silty clays, lean clays	CL	2500 to 6000 ^b	17 to 18 ^b
Inorganic clays of high plasticity	CH	1000 to 5500 ^b	3 to 16 ^b

Furthermore, multiple electrodes can be installed to reduce the earth electrode resistance further. The electrodes combined resistance decreases when the gap between electrodes is less than the electrode length. The combined resistance drops because of the electrode's high strength field. The combined resistance will only increase if the gap between electrodes is several rod lengths apart. Table 2.3 shows the multiplying factors for multiple electrodes from IEE 142 standard. To calculate the combined resistance, the electrode's actual total resistance is divided by the number of electrodes and multiplied with factor F.

Table 2.3: Multiplying factors for multiple electrodes (IEE 142, 2007)

Number of rods	F
2	1.16
3	1.29
4	1.36
8	1.68
12	1.80
16	1.92
20	2.00
24	2.16

2.4.3 Grounding Evaluation Methods

The grounding evaluation is a test to measure a grounding system's soil resistivity or total grounding resistance. There are six evaluation methods; each method has its working principle, application, pros and cons. Table 2.4 summarizes the characteristics of each evaluation method.

Table 2.4: Characteristics summary for grounding evaluation methods

Methods	Advantages	Disadvantages	Application	Earthing system size
Two Point Method	<ul style="list-style-type: none"> • Electrode under measured can stay connected to system. • Simplest way to obtain a ground resistance reading. • Requires less testing electrodes and small area for evaluation. 	<ul style="list-style-type: none"> • Has the lowest accuracy among the methods. • Only be used as a last resort. 	<ul style="list-style-type: none"> • Grounding resistance measurements. • Used where the driving of ground spike is neither practical nor possible. 	Small and moderate system.
Three Point Method	<ul style="list-style-type: none"> • Widely accepted and high accuracy. • Most reliable test method. • Quicker and simpler than Four Point Method. 	<ul style="list-style-type: none"> • Ground electrodes must be disconnected. • Time consuming and labor intensive. • Ineffective if the electrical center is unknown. 	<ul style="list-style-type: none"> • Grounding resistance measurements. • High electrical load. • Useful for homogeneous soil. 	Moderate and large system.
Four Point Method	<ul style="list-style-type: none"> • Widely accepted and high accuracy. • Quick and easy method. • Extremely reliable conforms to IEEE 81. 	<ul style="list-style-type: none"> • Ground electrodes must be disconnected. • Requires a large distance and spacing. • Time consuming and labor intensive. 	<ul style="list-style-type: none"> • Soil resistivity measurement. • Use for multiple depth testing. 	Moderate and large System.
Clamp-on test method	<ul style="list-style-type: none"> • High Accuracy. • Electrode under measured can stay connected to system. • No need to turn off the equipment power. • Not dangerous to human life. 	<ul style="list-style-type: none"> • Accuracy affected if frequency of AC current injected, • Cannot apply on isolated grounds • Low earth resistance (0.5Ω) is difficult with this method. 	<ul style="list-style-type: none"> • Grounding resistance measurements. • Only effective in situations with multiple earthing electrodes are in parallel and a closed circuit is available for the current circulation. 	Suitable for all systems.
Slope Method	<ul style="list-style-type: none"> • High Accuracy. 	<ul style="list-style-type: none"> • Requires calculation. 	<ul style="list-style-type: none"> • Grounding resistance measurements. • Sub-station earths and power station. 	Large system.
Star-Delta Method	<ul style="list-style-type: none"> • Suitable for rocky terrain area which have no suitable locations for installing test electrodes. 	<ul style="list-style-type: none"> • Requires calculation. 	<ul style="list-style-type: none"> • Grounding resistance measurements. • Rocky terrain area. 	Large system.

A new grounding system performs this evaluation so that areas with low soil resistivity can be discovered. The low soil resistivity reduces the installation cost because earth electrodes with low resistivity can be applied. Besides, the evaluation also determines the perfect spacing between multiple earth electrodes, which further reduces the grounding system earth resistance. Furthermore, the old grounding system also performs this evaluation for condition checking. The soil corrosion affects the earth electrode conditions and connections, causing the grounding system resistivity to increase. Thus, evaluating on time allows the poor earth electrode to be replaced and ensures the grounding system resistivity.

2.4.3.1 Two Point Method

The Two Point Method contains two connection points. It is the fastest but least accurate method among the evaluation methods. It measures the grounding resistivity of an earth electrode with an earth tester, connecting the earth

electrode to be tested (E) with the metallic grounding point. The distance for both grounding points ranges between 5 m or 10 m. Examples for metallic grounding point is transformers casing and metallic water pipe.

The earth tester used can be a three-terminal or four-terminal. As shown in Figure 2.33, for a four-terminal, the C1 and P1 terminals are interconnected with a jumper wire; this applies to the C2 and P2 terminals as well. Next, the C1 and the C2 terminal connect to E electrode and the metallic grounding point. The P and C terminals in the three-terminal are interconnected with a jumper wire. Next, the X and the C terminal connect to the E electrode and the metallic grounding point.

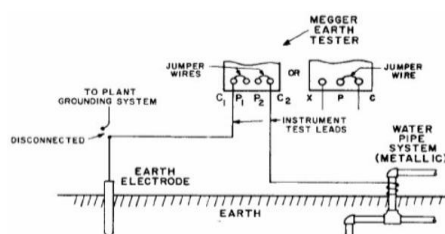


Figure 2.33: Two-Point Method

2.4.3.2 Three Point Method

The Three Point Method is a method applied to measure the grounding resistance value. This method applies two extra testing electrodes: the potential probe (P) and the current probe (C). It determines the perfect installation spot for the earth electrode (E) by measuring the grounding resistance on probe P.

Probe P is placed in the middle position between the C and E electrodes and connected to the P terminal for the connection. Next, probe C is placed 10 meters away from the E electrode and connected to the C terminal. With this connection, the earth tester will calculate the grounding resistance on probe P. Figure 2.34 illustrates the three-point method connection layout.

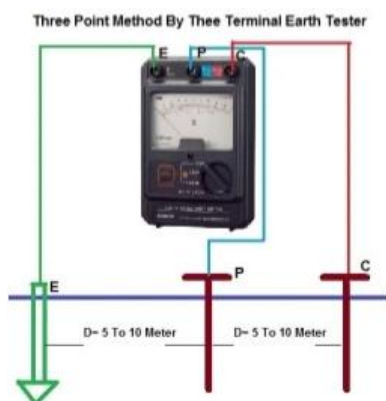


Figure 2.34: Three-Point Method (Electrical Notes & Articles, 2020)

However, the grounding resistance obtained by the earth tester is affected when electrodes E and C are close together. The effective resistance area on each electrodes E and C interfered together, affecting the resistance value calculated. As such, the distance for each probe P and C away from the electrode E will increase up to 10 meters and 15 meters until the earth tester obtains a resistance value. The resistance value of probe P and the distance of probe P away from electrode E are recorded and drawn in a graph. As shown in Figure 2.35, the constant pattern in the graph indicates the perfect installation spot for the earth electrode E. The perfect installation spot usually falls on 62% of the total distance between electrode E and C. Hence the three-point method is also known as the 62% method.

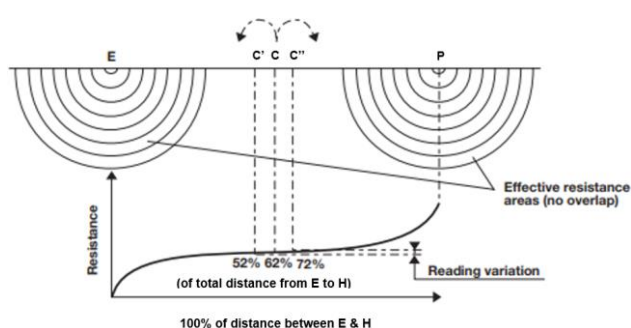


Figure 2.35: The effects of distance on electrode resistance

2.4.3.3 Four Point Method

The Four Point Method is the only soil resistivity measurement method among the evaluations. The electrode E must be disconnected from the grounding system for evaluation. Besides, a four terminal earth tester and three extra

testing electrodes: two potential probes (P1 and P2) and one current probe (C) are applied in this method. The gap between the electrodes must be 20 times greater than the depth of electrode E. The electrode E and probe C are placed at the outer side of the electrodes' arrangement. Both electrodes are connected with the current terminal of the earth tester for current injection. The current injected may be supplied from an AC or a DC source with a frequency ranging between 40 Hz to 100 Hz. Next, probes P1 and P2 are placed between the current electrodes and connected with the potential terminal of the earth tester. The earth tester calculates the potential difference between probe P1 and P2. Figure 2.36 illustrates the four-point method connection layout.

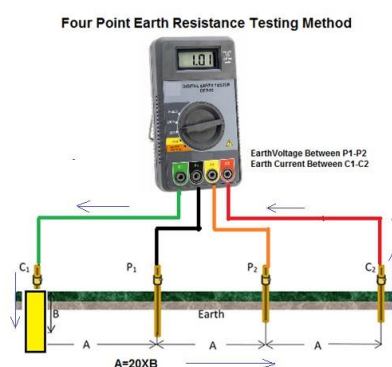


Figure 2.36: Four-Point Method (Electrical Notes & Articles, 2020)

With current and potential difference value recorded, the grounding resistance, R is calculated in the earth tester via the Ohm's Law

$$R_g = \frac{V_{p1p2}}{I_{ECA}} \quad (2.4)$$

Where:

R_g = grounding resistance, Ω

V_{p1p2} = potential difference between probe P₁ and P₂, V

I_{ECA} = current flow between electrode E and probe C, A

Next, the soil resistivity is calculated with the equation

$$\rho = 2\pi a R_g \quad (2.5)$$

Where:

ρ = soil resistivity, Ωm

a = gap between electrode in four-point method, m

R_g = grounding resistance, Ω

2.5 Harmonic

In electrical engineering, harmonic is known as the multiplication between the system's base frequency and the voltage or current. In other words, the shape or properties of the voltage or current waveform is influenced by the base frequency. Typically, in the alternating current (AC) system, the voltage or current waveform will be a pure sinusoidal wave. If these waveforms deviate from the sinusoidal wave, they contain harmonic. The existence of harmonics in the waveform is unwanted. They increase the base frequency and change the pure sinusoidal waveform by distorting the wave pattern. Hence, this situation is known as harmonic distortion.

2.5.1 Complex Waveform

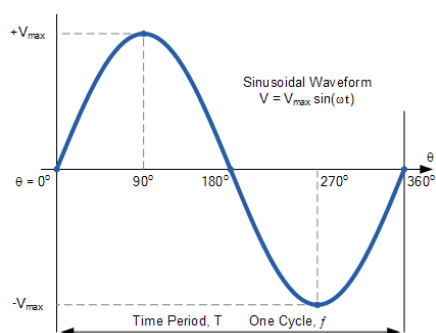


Figure 2.37: Fundamental waveform (electronicstutorials, n.d.)

As shown in Figure 2.37, a pure sinusoidal waveform containing the supply frequency is the fundamental waveform or first harmonic waveform. A second harmonic frequency will be formed when the base frequency is multiplied by two, likewise multiplying the base frequency with three and four forms the third and fourth harmonic frequencies. In short, harmonics are the multiplication of numbers with base frequencies and are written as $2f$, $3f$, $4f$, etc.

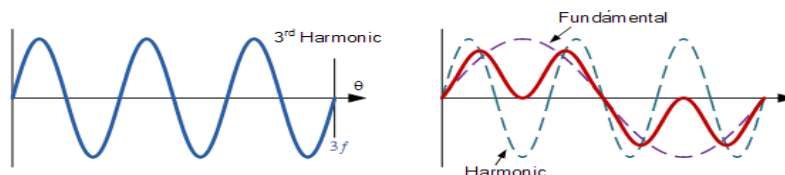


Figure 2.38: Formation of complex waveform (electronicstutorials, n.d.)

A complex waveform is created when the harmonic content is combined with the fundamental waveform. For example, in Figure 2.38, a complex waveform is created when the fundamental waveform and the third harmonic waveform merge. The forming of the complex waveform is based on the fundamental waveform phase and the frequency and the amplitude of the harmonic content.

2.5.2 Harmonic Sequencing

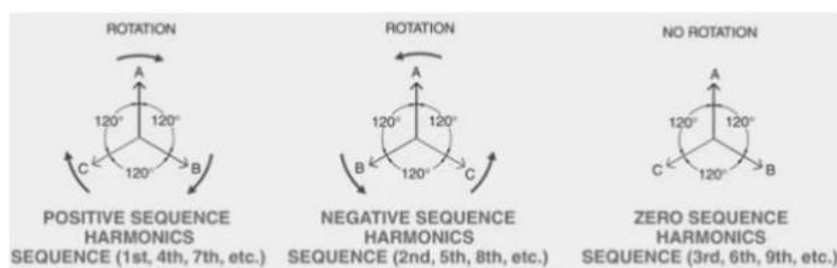


Figure 2.39: Rotating direction for the harmonic sequence

The harmonic sequence occurs when the network is powered in a balanced three-phase four-wire system. As shown in Figure 2.39, there are three types of harmonic sequence. These harmonic sequences are defined via the phasor rotating direction of the harmonics about the fundamental waveform.

The first type is known as the positive sequence harmonic. Harmonic frequencies such as the fourth, seventh and tenth are categorized as the positive sequence harmonic. The rotating direction for these frequencies and the fundamental waveform is the same. They rotate forward.

Secondly, the harmonic frequencies in the negative sequence harmonic are the second, fifth, and eighth. They rotate in a reverse direction, the opposite of the fundamental waveform rotating direction.

The last harmonic sequence is known as triplen harmonics and also zero-sequence harmonics. Since triplen is the multiple of three, harmonic

frequencies such as third, sixth, and ninth are in this category. Besides, these harmonic frequencies have one similarity: they are all shifted in the sequence of zero. Unlike the positive and negative sequence harmonic, the zero-sequence harmonic only rotates between the phase and neutral or ground.

2.5.3 Impacts of Harmonic Distortion

The existence of harmonic distortion is undesirable because it impacts the performance of the load, protection and switching device, and the utility that connects to the system network. This section provides a few examples of the impact of harmonic distortion.

The transformer performance is permanently reduced when there is harmonic distortion. This is because every harmonic sequence can cause an overheating effect on the transformer. For instance, when the load is affected by a positive sequence harmonic, the losses at the transformer, such as the resistance and the eddy current, will be increased. This will result in an overheating issue at the transformer when the losses mentioned above increase. These losses are released as heat. The voltage supplied to the load is affected as the power quality is affected by the power loss and overheating issue.

Secondly, the performance of protective equipment such as circuit breakers and fuses are also affected. This is because the harmonic distortion increases the RMS current value. The thermal-magnetic tripping mechanism of the circuit breaker is sensitive to the RMS current. As such, issue such as false tripping in a circuit breaker happens when there is a high RMS current value. Besides, when the RMS current is distorted, the high RMS current will cause a heating effect on the fuse. This will cause the fuse to act faster and burst.

Lastly, the performance and lifespan of the capacitor are also affected. The harmonic distortion will cause overheating, overloading, voltage stress, power losses, and increment of dielectrics at the capacitor. Besides, the harmonic distortion will create a harmonic resonance issue on the capacitor, reducing the power quality across the system.

CHAPTER 3

METHODOLOGY AND WORK PLAN

3.1 Introduction

In this project, all simulations are carried out on the Simulink program in the MATLAB Software. A surge waveform that follows the 1.2/50 combination waveform generator of the IEC 61000-4-5 standard is built. To study the performance of the SPD during surge fault, the generated surge waveform is applied, and the SPD device is connected to the earthing systems. Besides, the grounding impedance value of the earthing system is also varied, and the harmonic distortion is also applied to the system. The simulation duration applied throughout this project is 0.6 seconds.

3.2 Surge/ Combination Waveform Generator Model

This experiment's combined waveform generator model is an impulse generator RLC circuit. This circuit is supplied with a 1539 V direct current source and an 800 Ω charging resistor. The waveform generated by this circuit must comply with the 1.2/50 μs combined wave generator of the IEC 61000-4-5 standard. When open-circuited, the generated waveform must contain a 1.2 μs front and 50 μs tail time. If short-circuited, the generated waveform must contain an 8 μs front time and 20 μs tail time. The model is defined to generate the surge in 0.06 seconds. The front time and tail time of the simulated open circuit voltage waveform and short circuit current waveform are compared with the theoretical standard defined in the IEC 61000-4-5 standard. Figure 3.1 shows the combination waveform generator circuit applied in this experiment.

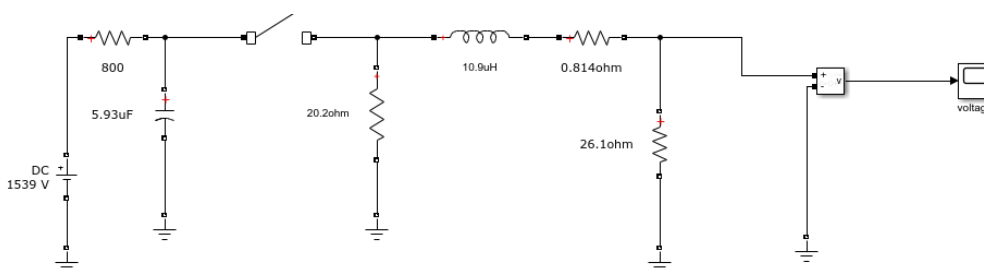


Figure 3.1: 1.2/50 μs combine wave generator circuit

3.3 Earthing System Network Model

The earthing system network model is created to allow surge to be applied. Due to the electrical component limitation in the Simulink software, only three earthing systems of the TT, IT, and TNC are designed. The earthing system network model is designed according to their electrical network characteristics.

Each of the earthing systems contains a -three phase AC source. This AC source includes an internal resistance and inductance of 0.5Ω and 2 mH . To reduce the project's complexity, the three-phase AC load connected to the earthing system is a pure 20Ω resistive load with an operating voltage value of 240 Vrms . The AC load's parameter will be remained fixed throughout the project. Besides, a three-phase series resistor of 20Ω is connected as well. This resistor acts as the grounding resistance for the earthing system. Figure 3.2 shows the circuit layout for three different earthing system network models with surge applied from the surge generator.

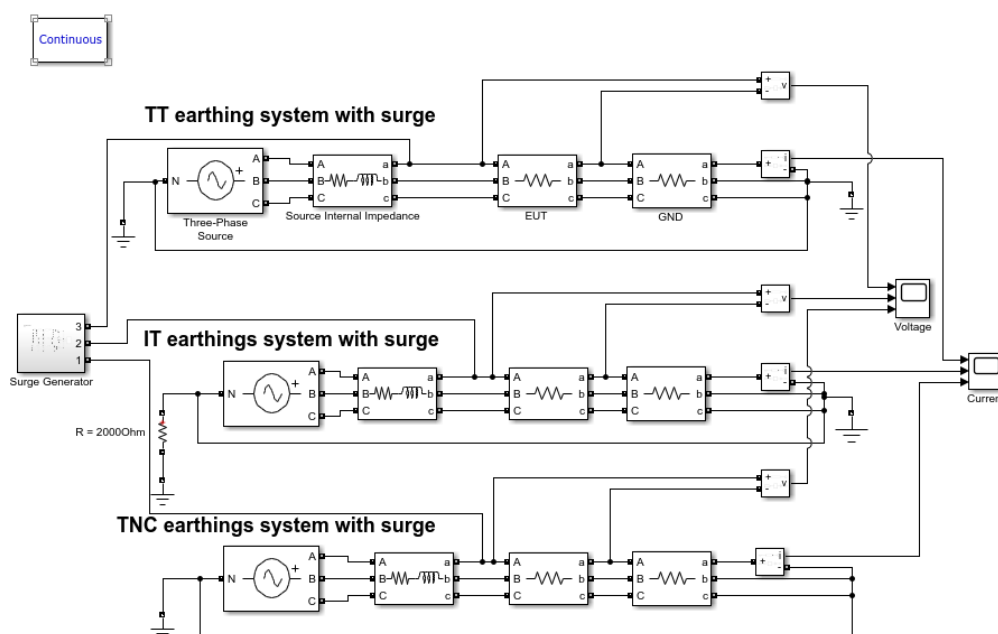


Figure 3.2: Surge applied on the earthing system network models

3.4 SPD

The experiment for conventional SPD (MOV) and power electronic SPD (MOSFET) is carried out separately. Each SPD is connected to all three earthing systems via common-mode protection. Since the three-phase series resistor acts as the grounding resistance, the SPD will be connected parallel to either one of

the AC load's phase lines instead of connecting to the ground. Figure 3.3 and Figure 3.4 show the circuit layout of the earthing system with MOV and MOSFET connected.

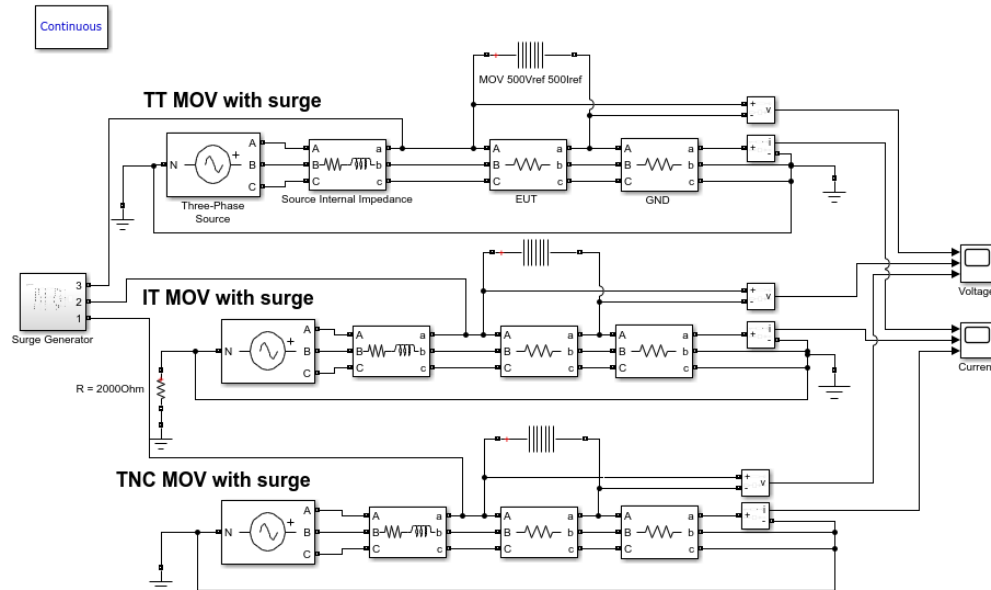


Figure 3.3: Connection of MOV in three earthing system network model

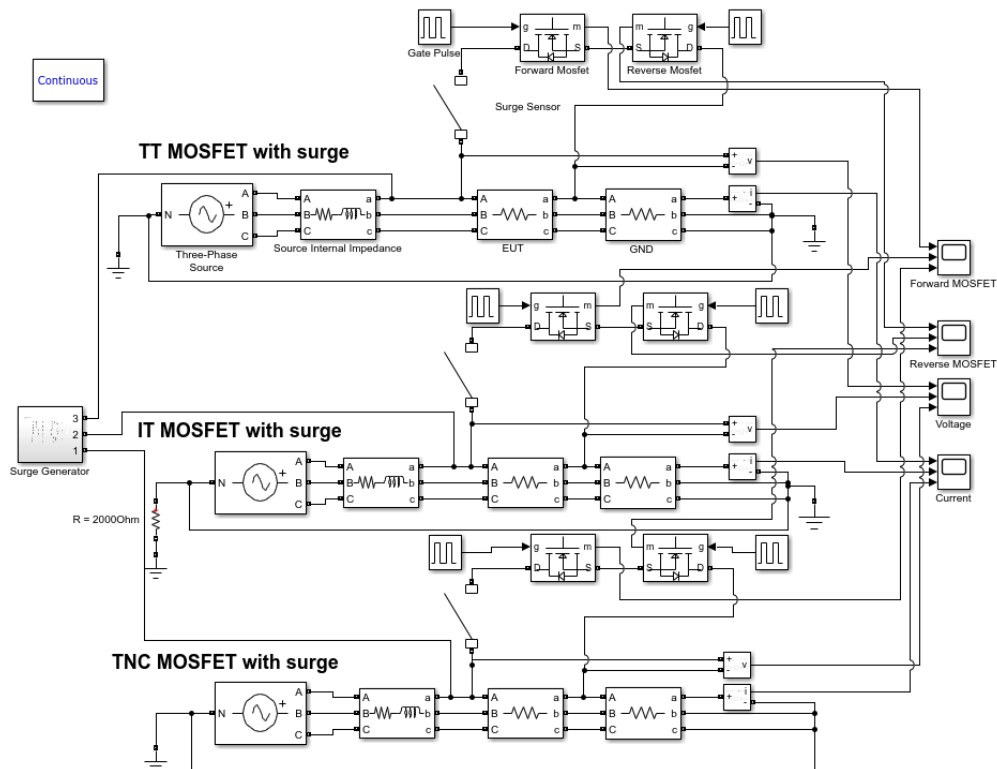


Figure 3.4: Connection of MOSFET in three earthing system network model

3.5 Grounding Impedance Deviation

To study the impact of grounding impedance deviation on the SPD performance, the resistance value of the three-phase series resistor is varied. The grounding resistance with a value of 20, 40, 60, 80 to 100 Ω is tested for MOV and MOSFET at all earthing systems. Figure 3.5 shows the simulation circuit for grounding impedance deviation on MOV performance at the different earthing systems.

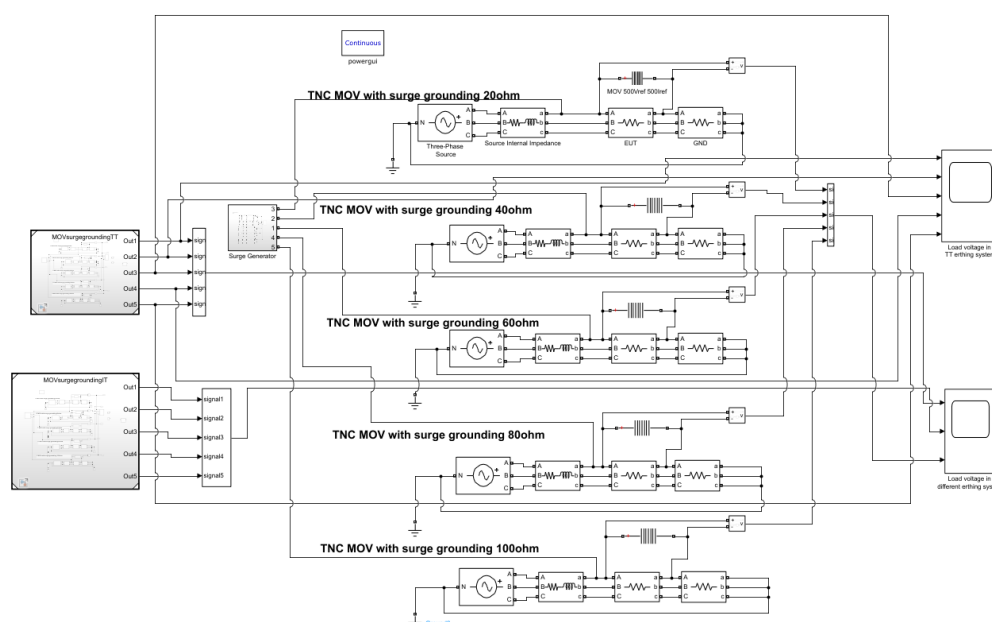


Figure 3.5: Simulation circuit for grounding impedance deviation at different earthing system with MOV connected

3.6 Harmonic Distortion (Triplen Harmonic)

To study the impact of harmonic distortion on the SPD performance during surge fault, a triplen harmonic signal is applied to each of the earthing system network models. The triplen harmonic signal is added to the network model by enabling the harmonic generation function in the three-phase AC source. The triplen harmonic's amplitude and phase are 0.41 pu and 0 degrees. Figure 3.6 shows the setting to enable the triplen harmonic generation in the three-phase AC source.

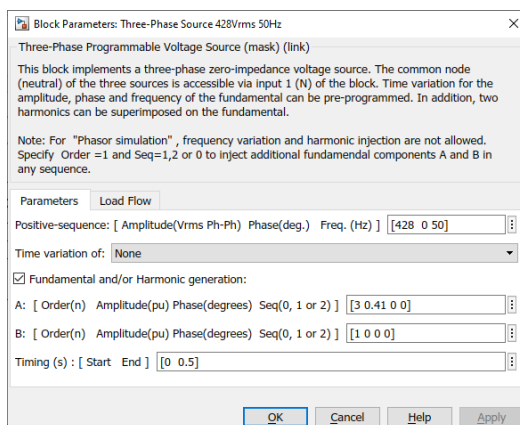


Figure 3.6: Setting for triplen harmonic generation via three-phase AC source.

3.7 Parameters to be study

After carrying out the simulation, the following parameters are used to evaluate the SPD's performance:

1. Response time
2. Fall time
3. Clamping value

The difference in network model waveform shape is also compared, allowing the impact of the different earthing systems and the impact of harmonic distortion on the SPD performance to be studied.

3.8 Workplan

Figure 3.7 shows the overall experiment and simulation flow in this project.

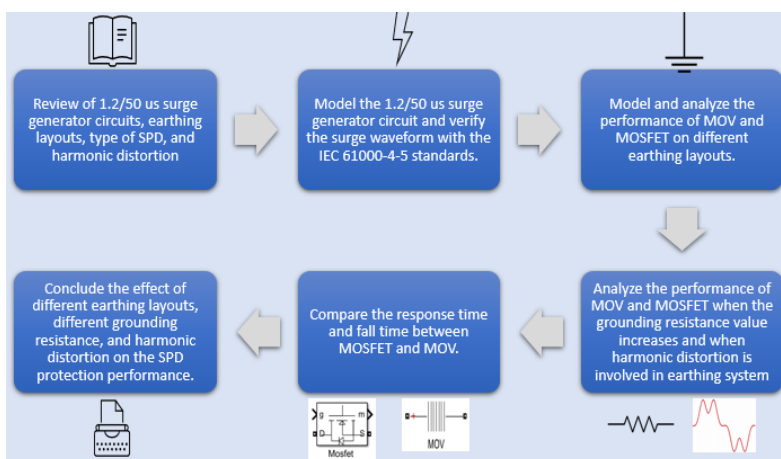


Figure 3.7: Experiment and simulation workplan

CHAPTER 4

RESULTS AND DISCUSSION

4.1 Introduction

This chapter explains the simulated result for the surge generator and the earthing system models. Furthermore, the SPD device's (MOV and MOSFET) performance with different earthing system models, grounding impedance deviation, and triplen harmonics are discussed.

4.2 Surge / Combination Wave Generator Model

Since the components value in the surge generator circuit is unknown, equations are created to obtain these unknown values to allow simulation. Next, the simulated open-circuit voltage waveform and short-circuit current waveform are compared with the IEC 61000-4-5 standard.

4.2.1 Derivation for Open Circuit Voltage formula

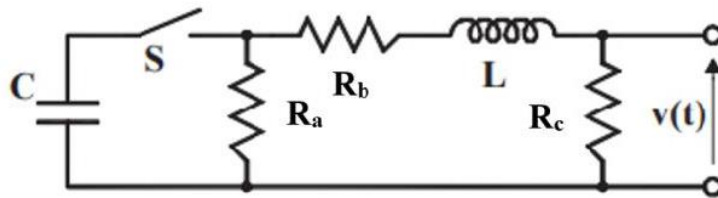


Figure 4.1: IEC 61000-4-5 1.2/50 μ s open circuit voltage design

A Laplace Transform equation for the output voltage is created below. This equation refers to the IEC 61000-4-5 1.2/50 μ s open circuit voltage design as depicted in Figure 4.1.

$$V(s) = \frac{E \frac{R_c}{L}}{s^2 + s \left(\frac{R_a + R_b}{L} + \frac{1}{R_a C} \right) + \frac{R_a + R_b + R_c}{R_a L C}} \quad (4.1)$$

At the denominator, the Sum of Roots and the Products of Roots can be written as Equations 4.2 and 4.3.

$$\alpha + \beta = \frac{R_a + R_b}{L} + \frac{1}{R_a C} \quad (4.2)$$

$$\alpha\beta = \frac{R_a + R_b + R_c}{R_a L C} \quad (4.3)$$

$$V(s) = \frac{\frac{E R_c}{L}}{s^2 + s(\alpha + \beta) + \alpha\beta} \quad (4.4)$$

The simplified equation is inverted from the Laplace-domain function into the time domain function.

$$V(t) = \frac{E R_c}{\beta - \alpha} (e^{-\alpha t} - e^{-\beta t}) \quad (4.5)$$

The duration to achieve maximum voltage is calculated as

$$t_{pv} = \frac{\ln(\beta/\alpha)}{\beta - \alpha} \quad (4.6)$$

With Equation 4.6, the maximum voltage equation is equivalent to

$$V_{max} = \frac{E R_c}{\beta - \alpha} (e^{-\alpha t_{pv}} - e^{-\beta t_{pv}}) \quad (4.7)$$

4.2.2 Derivation for Short Circuit Current formula

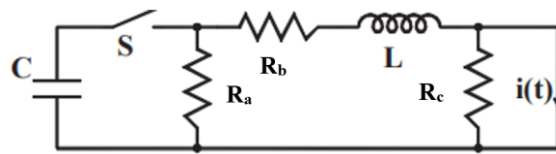


Figure 4.2: IEC 61000-4-5 8/20 μ s short circuit voltage design

A Laplace Transform equation for the short circuit current is created below. This equation refers to the IEC 61000-4-5 1.2/50 μ s short circuit current design as depicted in Figure 4.2.

$$I(s) = \frac{E/L}{s^2 + s\left(\frac{R_b}{L} + \frac{1}{R_a C}\right) + \frac{R_a + R_b}{R_a L C}} \quad (4.8)$$

At the denominator, the Sum of Roots and the Products of Roots can be written as Equations 4.9 and 4.10.

$$\omega_o^2 = \frac{R_a + R_b}{R_a L C} \quad (4.9)$$

$$\frac{\omega_o}{Q} = \frac{R_b}{L} + \frac{1}{R_a C} \quad (4.10)$$

$$\omega_n = \omega_o \sqrt{1 - \left(\frac{1}{2Q}\right)^2} \quad (4.11)$$

By using Equation 4.11, the simplified equation for Equation 4.8 and the Laplace inversed equation are written as

$$I(s) = \frac{E/L}{(s + \omega_o/2Q)^2 + \omega_n^2} \quad (4.12)$$

$$i(t) = \frac{E}{\omega_n L} e^{\frac{\omega_o}{2Q}t} \sin(\omega_n t) \quad (4.13)$$

With the duration to achieve maximum current equation, the maximum current equation is written as

$$t_{pc} = \frac{1}{\omega_n} \tan^{-1} \left(\sqrt{(2Q)^2 - 1} \right) \quad (4.14)$$

$$I_{max} = \frac{E}{\omega_o L} e^{\frac{\omega_o}{2Q}t_{pc}} \quad (4.15)$$

4.2.3 Derivation for parameter formula

According to Carobbi (2013), the resistor, R_c , can be calculated by dividing the maximum voltage, V_{max} , and I_{max} 's maximum current. Besides, by assuming $R = 2 \Omega$ and $V_{max} = I_{max}R$, the R_c is derived into Equation 4.17.

$$R = \frac{V_{max}}{I_{max}} = \frac{\omega_o}{\beta - \alpha} \left(e^{-\alpha t_{pv}} - e^{-\beta t_{pv}} \right) e^{\frac{\omega_o}{2Q}t_{pc}} R_c \quad (4.16)$$

$$R_c = \frac{\beta - \alpha e^{-\frac{\omega_o}{2Q}t_{pc}}}{\omega_o \left(e^{-\alpha t_{pv}} - e^{-\beta t_{pv}} \right)} R \quad (4.17)$$

The remaining parameters are derived by simplifying Equations 4.2, 4.3, 4.9 and 4.10.

$$\frac{R_a+R_b}{L} + \frac{1}{R_a C} - \alpha - \beta = 0 \quad (4.18)$$

$$\frac{R_a+R_b+R_c}{R_a L C} - \alpha \beta = 0 \quad (4.19)$$

$$\frac{R_a+R_b}{R_a L C} - \omega_o^2 = 0 \quad (4.20)$$

$$\frac{R_b}{L} + \frac{1}{R_a C} - \frac{\omega_o}{Q} = 0 \quad (4.21)$$

$$L = \frac{R_c}{\alpha + \beta - \frac{\omega_o}{Q}} \quad (4.22)$$

$$R_b = \left(\frac{\omega_o^2}{Q} - \frac{\alpha \beta - \omega_o^2}{\alpha + \beta - \frac{\omega_o}{Q}} \right) L \quad (4.23)$$

$$R_a = \frac{\omega_o^2}{\alpha \beta - \omega_o^2} R_c - R_b \quad (4.24)$$

$$C = \frac{1}{R_a} \frac{\alpha + \beta - \frac{\omega_o}{Q}}{\alpha \beta - \omega_o^2} \quad (4.25)$$

In the Equation of 4.17 and 4.22 to 4.25, the constants of $\alpha = 14.662k$, $\beta = 2.463M$, $Q = 1.46$, and $\omega_o = 40060\pi$ are replaced for calculating the parameters value. As such,

$$R_a = 20.2 \Omega$$

$$R_b = 0.814 \Omega$$

$$R_c = 26.1 \Omega$$

$$C = 5.93 \mu F$$

$$L = 10.9 \mu H$$

4.2.4 Results for circuit and waveform

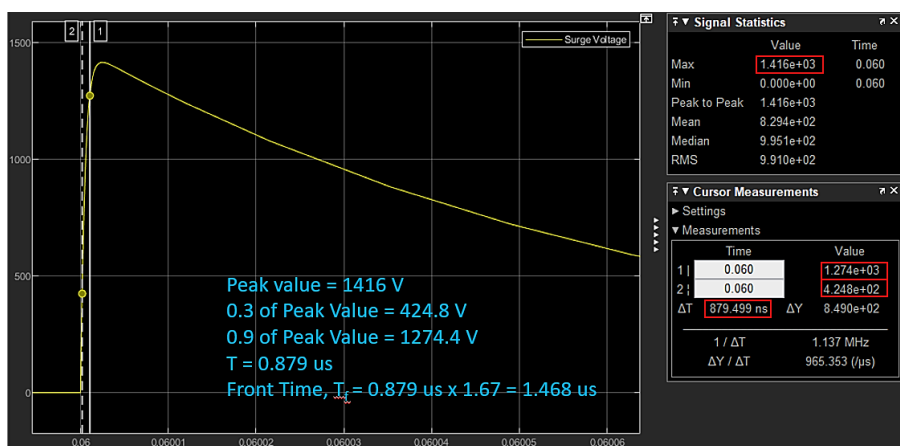


Figure 4.3: Open-circuit voltage waveform with front time at 1.469 μs

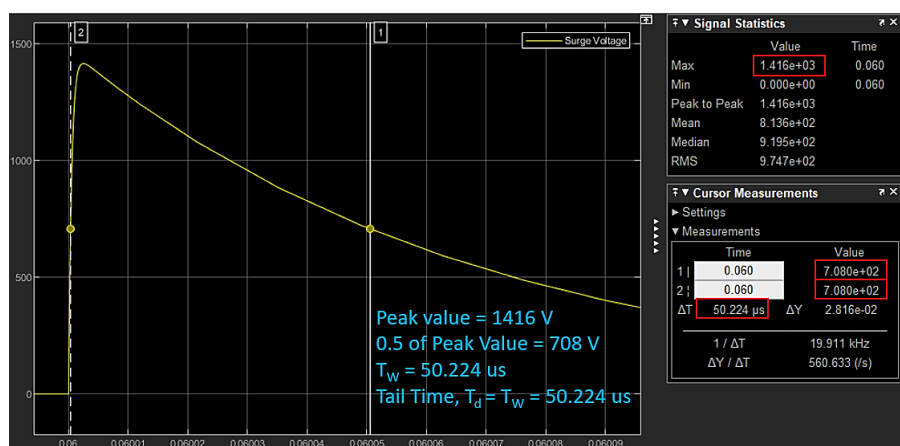


Figure 4.4: Open-circuit voltage waveform with tail time at 50.327 μs

Table 4.1: Percentage error for the simulated open-circuit voltage waveform

	Theoretical Value	Experimental Value	Percentage Error (%)
Front Time (μs)	1.2	1.468	22.33
Tail Time (μs)	50	50.224	0.448

Figure 4.3 and Figure 4.4 show the method for calculating the front time and tail time for the open-circuit voltage waveform. The calculation method applied for the front time and tail time is based on the IEC 61000-4-5. Both figures show that the open-circuit voltage waveform's front time and tail time are 1.468 μs and 50.224 μs . By comparing the simulated results with the IEC 61000-4-5 excellent value, it is found that the percentage error for both is still acceptable. Although the percentage error for the front time has a very high value of 22.33%,

it did not exceed the 30% limit defined by the standard. Thus, it is proven that the surge generator circuit applied in this project complies with the open-circuit voltage waveform standard in IEC 61000-4-5.

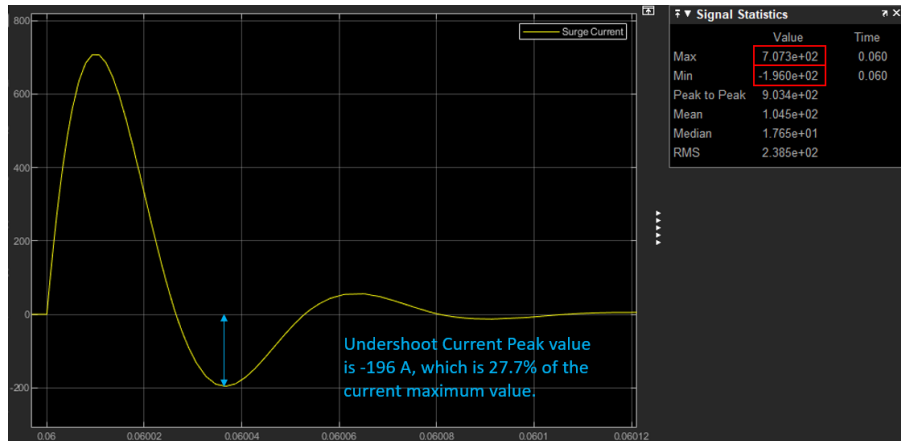


Figure 4.5: Short-circuit current waveform with undershoot peak value -196 A

According to the IEC 61000-4-5, the undershoot peak value for the short circuit current waveform must not be more excellent than 30% of the maximum waveform value. The generated short circuit current waveform in Figure 4.5 complies with this requirement as the undershoot peak value is -196 A, which is only 27.7% of the current maximum value.

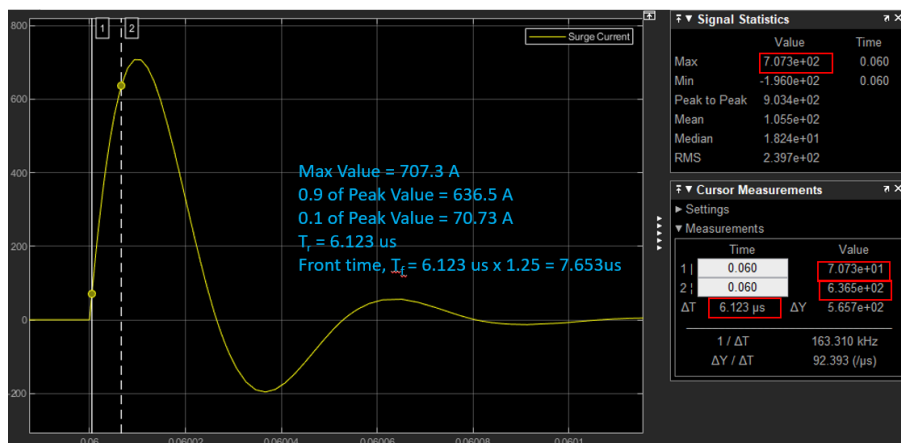


Figure 4.6: Short-circuit current surge waveform with front time at 7.653 μ s

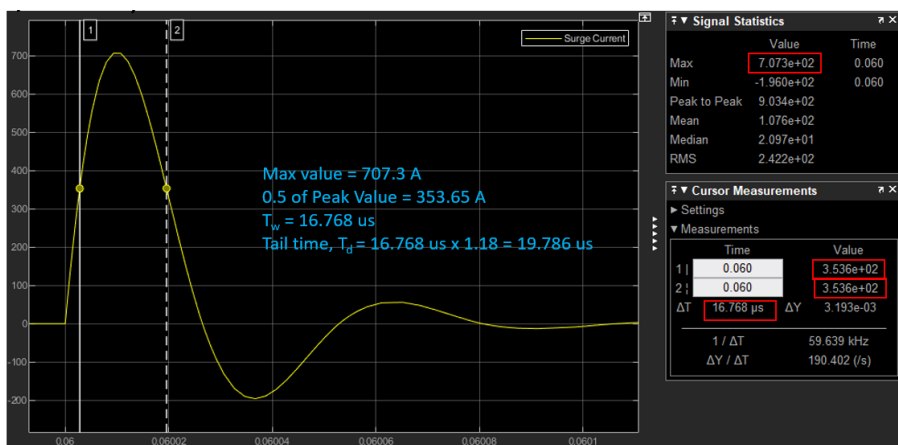


Figure 4.7: Short-circuit current surge waveform with tail time at 19.786 μs

Table 4.2: Percentage error for the simulated open-circuit voltage waveform

	Theoretical Value	Experimental Value	Percentage Error (%)
Front Time (μs)	8	7.653	4.33
Tail Time (μs)	20	19.786	1.07

The short-circuit current waveform's front time and tail time are 7.653 μs and 19.786 μs, as shown in Figures 4.6 and 4.7. Based on Table 4.2, it is found that the front time and tail time of the generated short circuit current waveform are very close to the excellent value set by the IEC 61000-4-5. Hence, it is proven that the surge generator circuit applied in this project fully complies with the IEC 61000-4-5.

4.3 Different earthing system with surge applied

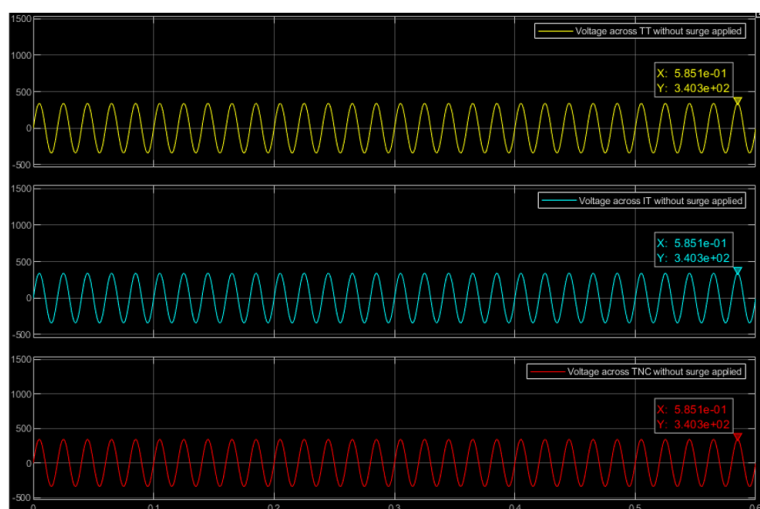


Figure 4.8: Load voltage waveform in different earthing systems

Table 4.3: Percentage error of the V_{rms} for the load

	Ideal Value (V_{rms})	Simulated Value (V_{rms})	Percentage Error (%)
V_{rms} of Load	240	240.6	0.261

Based on Figure 4.8, the load voltage in all three earthing systems contains a sinusoidal voltage waveform with the same peak value of 340.3 V. The load ideal operating voltage defined for this project is 240 Vrms. Since the sinusoidal voltage waveform, the peak value, V_{peak} is 340.3 V, this peak value is converted into V_{rms} via the formula:

$$V_{rms} = \frac{V_{peak}}{\sqrt{2}} \quad (4.26)$$

Based on Table 4.3, the load simulated in all systems contains 240.6 Vrms, which is acceptable as it is close to the ideal value and has a deficient percentage error.

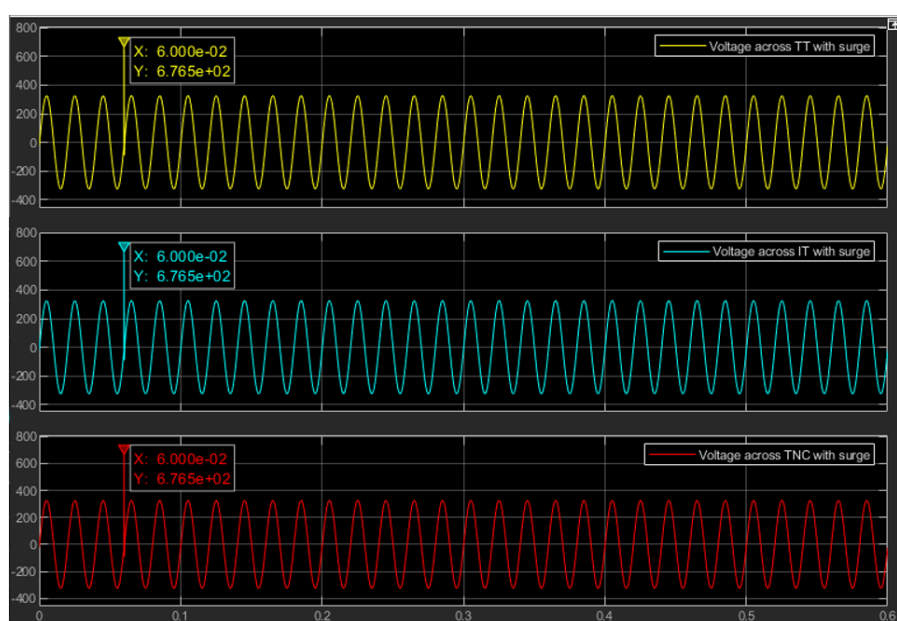


Figure 4.9: Load voltage waveform with surge in different earthing systems

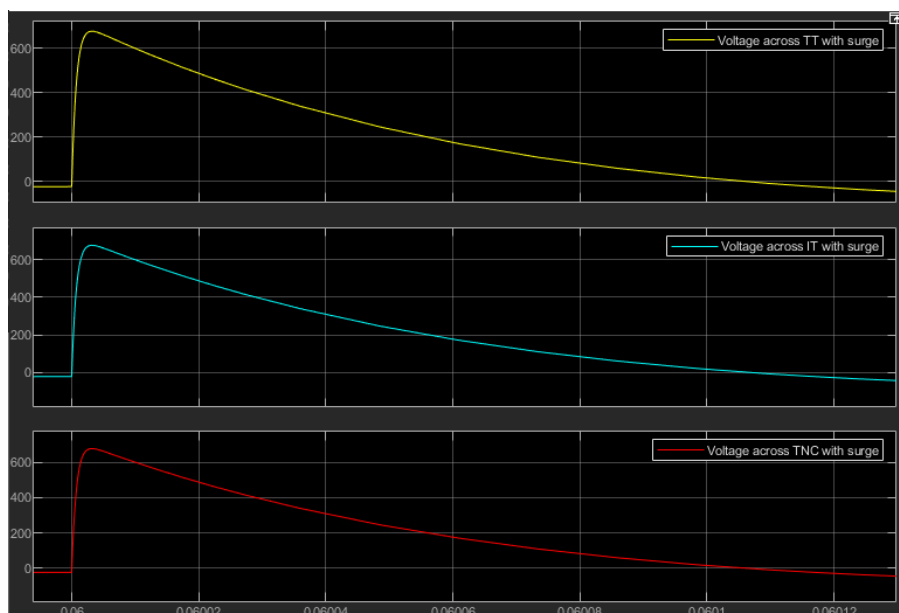


Figure 4.10: Overvoltage surge waveform in different earthing systems

The surge generator is set to generate the surge at 0.06 seconds. As shown in Figure 4.9, a spike of 676.5 V is formed on the load voltage's sinusoidal waveform when the surge is applied for 0.06 seconds. The voltage waveform across the load remains sinusoidal with V_{peak} at 340.3 V after the voltage spike due to the surge. The voltage spike waveform pattern in Figure 4.10 is like the open-circuit voltage waveform pattern in Figure. The earthing system voltage spike is lower than the purely generated voltage spike of 1416 V because the impedance across the earthing system has reduced the voltage spike value in the earthing system. However, with the voltage spike surging to 676.5 V, the load connected to the earthing system will still be damaged as the maximum voltage that the 240.6 Vrms load can accept is only 340.3 V. Hence, SPD must be installed to protect the load.

4.4 MOV Performance

This section focuses on discussing the protection efficiency of the MOV in the different earthing systems against the power surge. Firstly, the clamping performance of the MOV and the clamped waveform are discussed and compared. Next, the MOV reaction speed is evaluated by calculating the response time and the fall time. Lastly, the effect of different grounding resistance on the MOV performance in the different earthing systems is

evaluated by comparing the waveform, clamping performance, response time, and fall time.

4.4.1 Voltage clamped by MOV in different earthing system

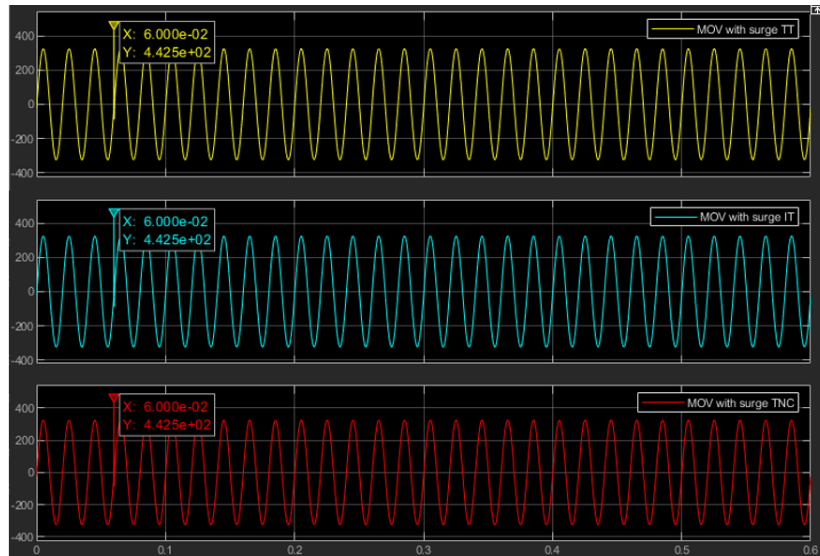


Figure 4.11: Load voltage waveform with MOV clamped surge in different earthing systems

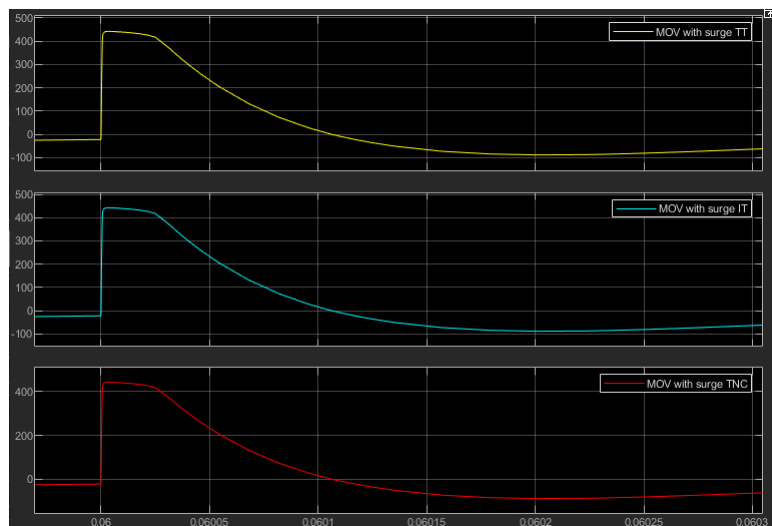


Figure 4.12: MOV clamped surge waveform in different earthing systems

As shown in Figure 4.11, all earthing systems have the same MOV peak clamping voltage value of 442.5 V. Based on Figure 4.12, the voltage spike waveform in the earthing systems are all similar. This shows that MOV clamping performance is not affected by the type of earthing system as the clamped voltage spike waveform and peak clamping value are all similar.

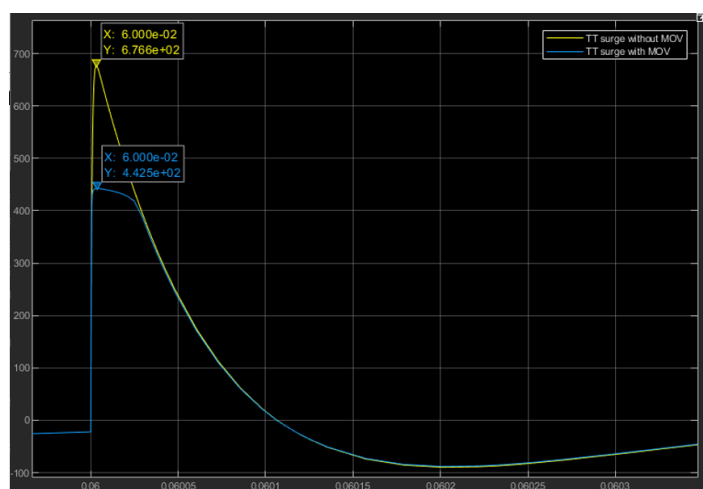


Figure 4.13: MOV clamped and unclamped surge waveform in TT earthing systems

As shown in Figure 4.13, an earthing system without the MOV will have its peak voltage spike value remains at 676.6 V. With the MOV connected, the voltage spike value is clamped down to 442.5 V. This is because the reference voltage of the MOV is set at 500 V. When the voltage across the MOV goes above 500 V, the high internal resistance of the MOV reduces significantly. This creates a short circuit path, allowing the voltage above 500 V to diverge to the ground. The MOV protects the load by clamping off any voltage spike beyond 500 V, ensuring the load will not be damaged during a surge event. The clamped voltage value is at 442.5 V instead of the ideal 500 V. This may be due to the built-in MOV's over-reduced internal resistance.

4.4.2 Response Time and Fall Time of MOV in different earthing system

To study the reaction time of the MOV during a surge event, the response time and the fall time of the MOV are calculated. Since all earthing systems with MOV connected have the same clamping performance and clamped waveform, the response time and the fall time of the MOV in the different earthing systems are also similar. Thus, this sub-section only shows the calculation method for the response time and fall time of the MOV at the TT earthing system.

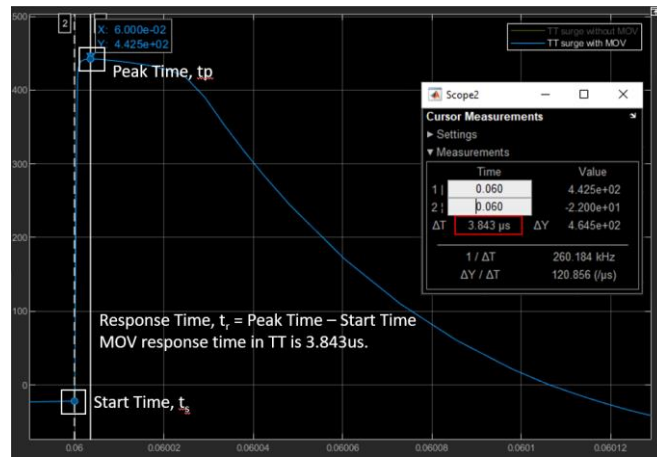


Figure 4.14: Measurement of the response time of MOV in TT earthing system

Figure 4.14 shows the method applied to measure the MOV's response time. Based on Figure 4.14, the response time of the MOV during a surge event is 3.843 μs . The response time is the duration for the MOV to react in clamping off the voltage spike. The response time for the MOV is calculated by finding the duration between the time taken to reach the peak clamped value and the start-up time. The formula to calculate the response time is shown below:

$$t_r = t_p - t_s \quad (4.27)$$

Where:

t_p : time taken to reach the peak clamped value

t_s : start up time

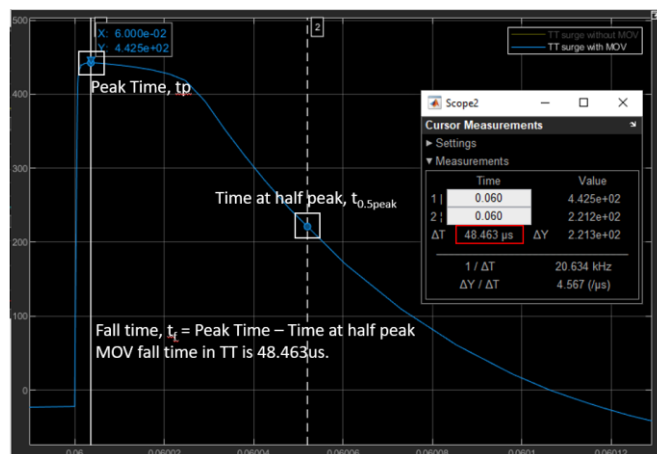


Figure 4.15: Measurement of the fall time of MOV in TT earthing system

Figure 4.15 shows the method applied to calculate the MOV's fall time. As shown in Figure 4.15, the fall time of the MOV during a surge event is 48.463 μ s. The fall time is the time taken for the MOV to fall from the peak clamped value to half of the peak clamped value. The formula to calculate the fall time is shown below:

$$t_f = t_{0.5peak} - t_p \quad (4.27)$$

Where:

$t_{0.5peak}$: time taken to reach half of the peak clamped value

t_p : time taken to reach the peak clamped value

4.4.3 Impact of grounding resistance value on MOV performance

This experiment is to study the impact of various grounding resistance values on the MOV performance in the different earthing systems. Figure 4.16 shows the voltage waveform across the AC load for the different earthing systems. As shown in Figure 4.16, the clamped voltage spike waveform and the sinusoidal waveform across the AC load are the same for all earthing systems when the grounding resistance increases from 20 Ω to 100 Ω .

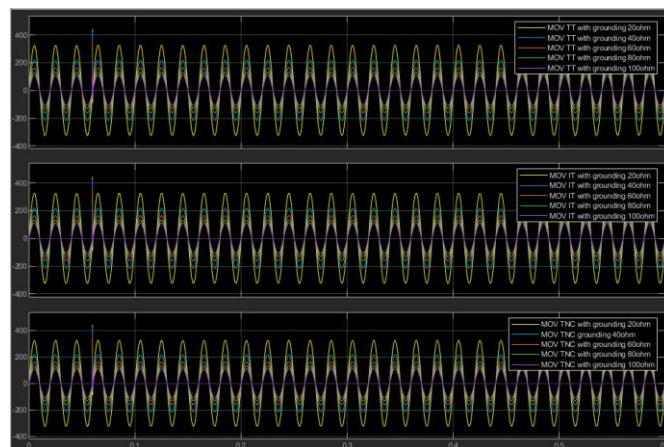


Figure 4.16: Load voltage waveform with MOV when grounding resistance increases

By taking a closer view of the clamped voltage spike waveform, all earthing systems have the same waveform patterns and trends. When the

grounding resistance in all three earthing systems increases, the peak of the clamped voltage spike waveform in these systems reduces.

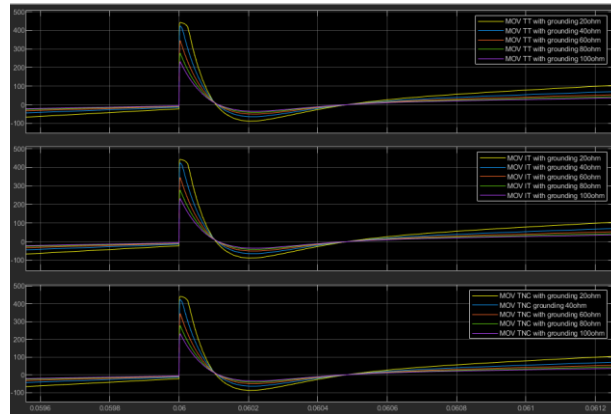


Figure 4.17: Load voltage waveform when grounding resistance increases

As shown in Figure 4.17, since these systems has similar MOV clamping voltage waveform when the grounding resistance increases, the impact of the grounding resistance value on the TT earthing system will only be studied.

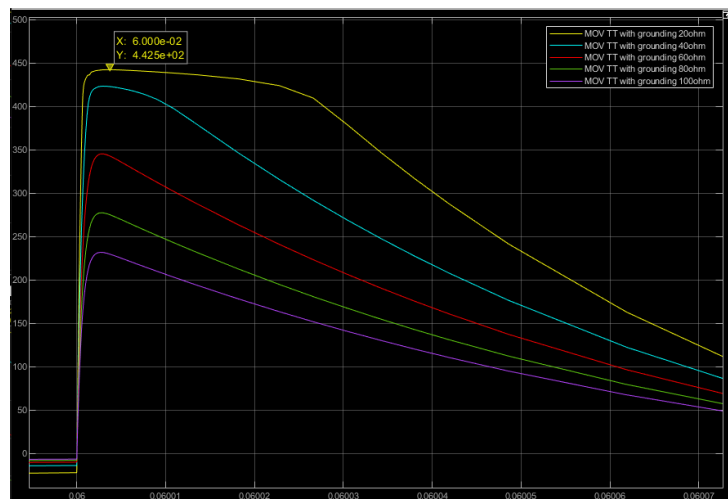


Figure 4.18: MOV clamped waveform when grounding resistance increases

Table 4.4: Summary of the MOV protection parameter in different grounding resistance

Grounding Resistance (Ω)	Peak clamping voltage of MOV (V)	Response Time, t_{res} (μs)	Fall Time, t_{fall} (μs)
20	442.5	3.843	48.463
40	423.5	3.016	37.045
60	345.5	2.740	36.051
80	277.6	2.664	35.033
100	232.0	2.650	34.897

As shown in Figure 4.18 and Table 4.4, the peak clamping voltage of the MOV decreases when the grounding resistance value increases. This implies that the MOV will clamp off more voltage to the ground when the grounding resistance increase. The measuring method in Figure 4.14 and Figure 4.15 calculates the response time and fall time. Based on the Table, the increase in the grounding resistance reduces the response time of the MOV. The MOV clamps away from the surge faster with higher grounding resistivity. In comparison, the fall time of the MOV reduces when the grounding resistance increase. This result shows that the internal resistance of the MOV that was decreased nearly to zero returns back to high resistivity quicker when the grounding resistivity increases.

The results above interpret that the performance of the MOV is not affected by the increasing grounding resistivity. This is because the objective of an ideal SPD is to clamp off as much surge waveform as it can. Besides, an SPD with a fast response time and fall time is more desirable. A faster response time allows the surge waveform to be diverted towards the SPD quicker and prevents any surge from damaging the load. Furthermore, a fast fall time allows the surge to be diverted to the ground quicker and allows the protected load to return to normal operating conditions faster.

4.5 MOSFET Performance

The MOSFET performance towards power surge in the different earthing systems is discussed in this section. Firstly, the difference between the MOSFETs and the load voltage waveform with and without surge for all earthing systems is discussed. Next, the MOSFET reaction speed in the different

earthing systems is studied. Lastly, the impact of different grounding resistance on the MOSFET performance for the earthing system is evaluated by comparing the waveform, clamping performance, response time, and fall time.

4.5.1 MOSFET waveform during surge event

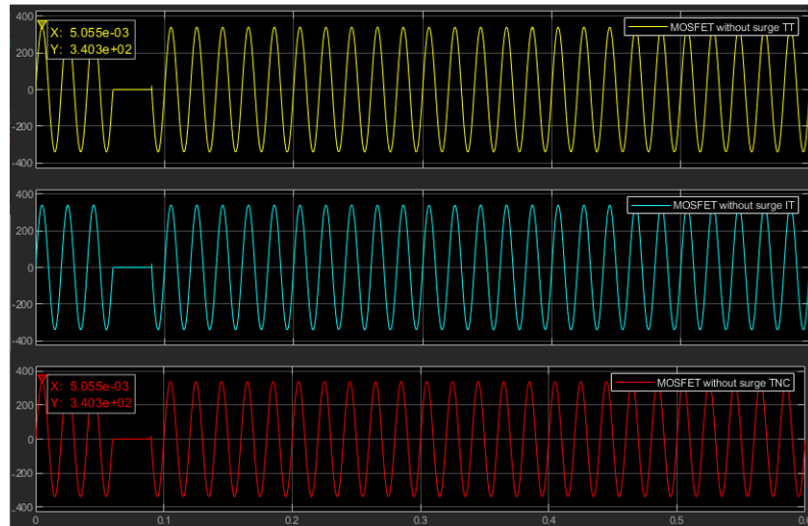


Figure 4.19: Load voltage waveform with MOSFET in different earthing systems

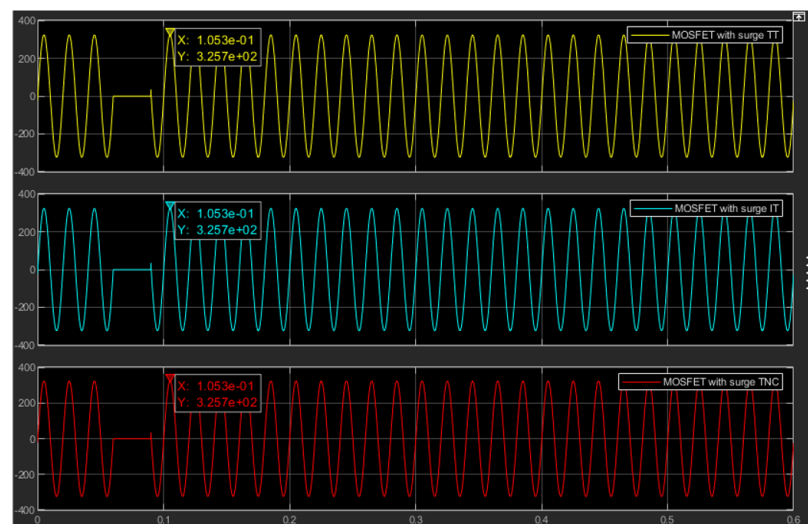


Figure 4.20: Load voltage waveform with MOSFET and surge in different earthing systems

To find the difference in the AC load voltage for all three earthing systems with MOSFET connected, the voltage waveform with and without surge applied are studied. From Figure 4.19, without surge applied, the load voltage peak value

remains for all earthing systems are similar at 340.3 V. This shows that the load operating voltage of 240 Vrms is not affected by the connected MOSFET. Based on Figure 4.20, the load voltage waveform in all earthing systems remains similar when the surge is applied. However, the AC load voltage peak value has decreased from 340.3 V to 325.7 V. This is due to the high open-circuit surge voltage that distorts the supplying voltage of the three-phase source. The sinusoidal waveform between 0.06 seconds and 0.085 seconds was missing. The MOSFET is defined as turning on at 0.06 seconds when the surge is applied. Hence, it clamps away the voltage supplied to the load within this period.

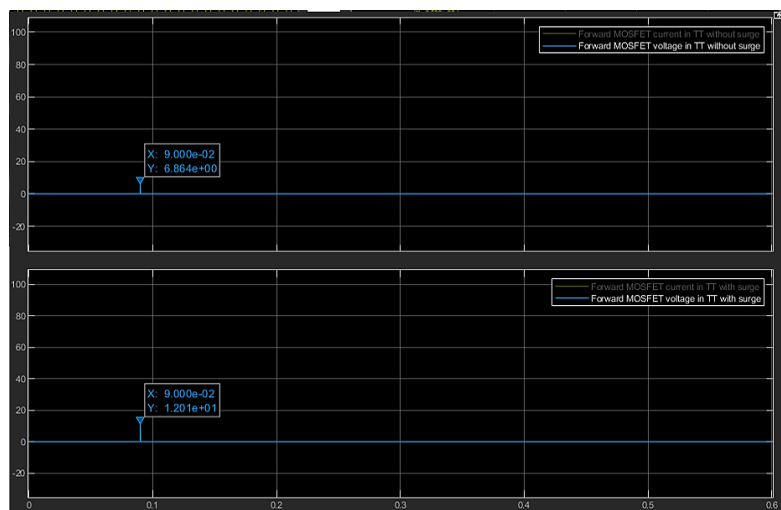


Figure 4.21: Switching transient waveform of forward MOSFET with and without surge

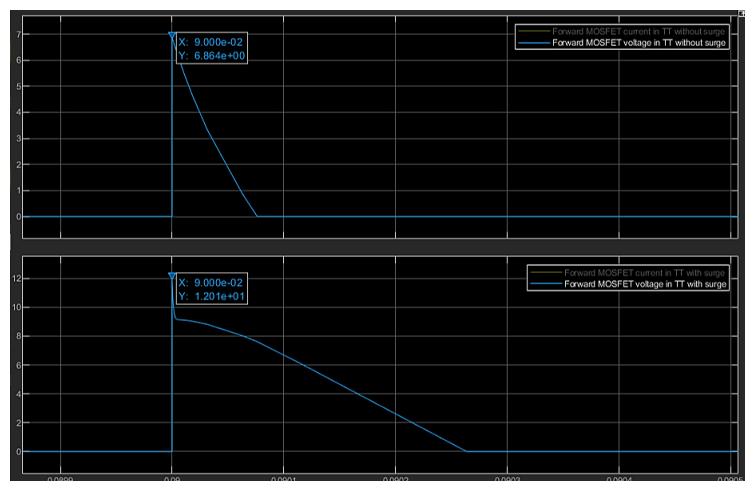


Figure 4.22: Zoom in view of forward MOSFET switching transient waveform

Since the load voltage waveform and peak value in all earthing systems are the same, this section will only study the forward MOSFET and reverse MOSFET performance in the TT earthing system. Figures 4.21 and 4.22 show the spike voltage waveform caused by the forward MOSFET switching off. When the surge is applied, the switch-off voltage peak value reduces from 68.64 V to 12.01 V. As shown in Figure 4.22, the forward MOSFET voltage waveform contains a transient characteristic. This causes the forward MOSFET to switch off slower during the surge event. This is acceptable as the surge applied distorts and reduces the voltage supplied to the forward MOSFET.

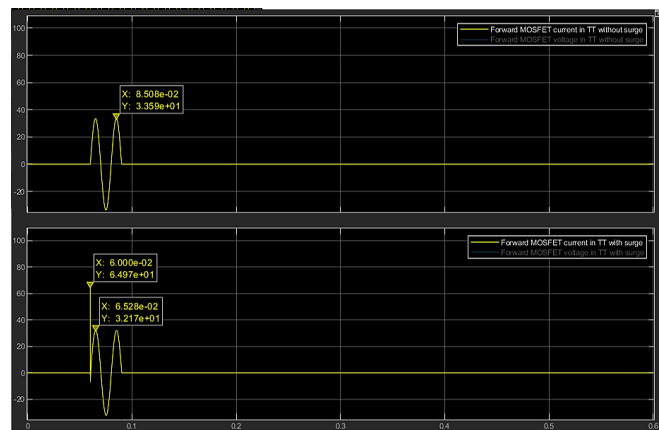


Figure 4.23: Operating current waveform of forward MOSFET with and without surge

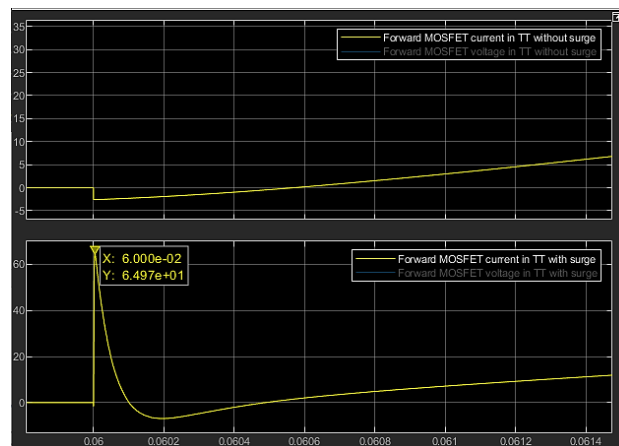


Figure 4.24: Zoom in view of forward MOSFET operating current waveform

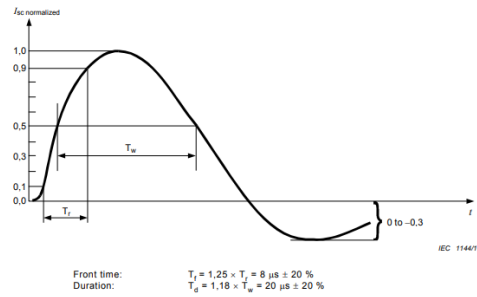


Figure 4.25: 8/20 μs short circuit current waveform (IEC 61000-4-5, 2014)

By observing Figure 4.23, there is a spike with a peak value of 64.97 A at the forward MOSFET current waveform when a surge is applied. Besides, due to the surge, the peak value of the forward MOSFET's operating current reduces from 33.59 A to 32.17 A. By comparing the spike waveform in Figure 4.24 with the ideal 8/20 μs short-circuit current waveform in Figure 4.25, both waveforms have the same shape. Thus, the presence of the spike waveform proves that the forward MOSFET clamps the surge current.



Figure 4.26: Voltage of reverse MOSFET with and without surge



Figure 4.27: Operating current waveform of reverse MOSFET with and without surge

Based on Figure 4.26, there are no changes to the reverse MOSFET voltage waveform as the voltage value remains at 0 V when the surge is applied to the earthing system. Besides, similarly to the current waveform of the forward MOSFET, a negative spike occurs in the reverse MOSFET. This shows the importance of using two MOSFET in the earthing system, as both MOSFET is needed to divert the surge waveform in the earthing system. Figure 4.27 shows the operating current waveform of reverse MOSFET with and without surge

4.5.2 Response Time and Fall Time of MOSFET in different earthing system

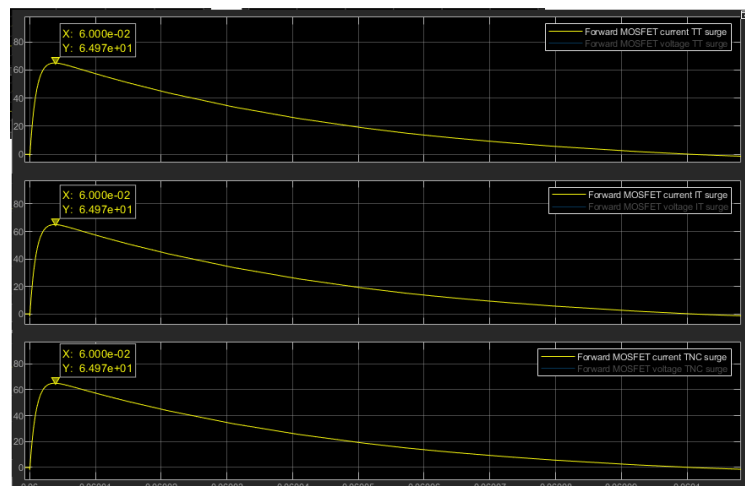


Figure 4.28: Forward MOSFET surge current waveform for different earthing system

As shown in Figure 4.28, the peak value of the spike measured in the forward MOSFET of all earthing systems has the same value of 64.97 A. The response time and the fall time of the forward MOSFET of the TT earthing system will only be calculated.

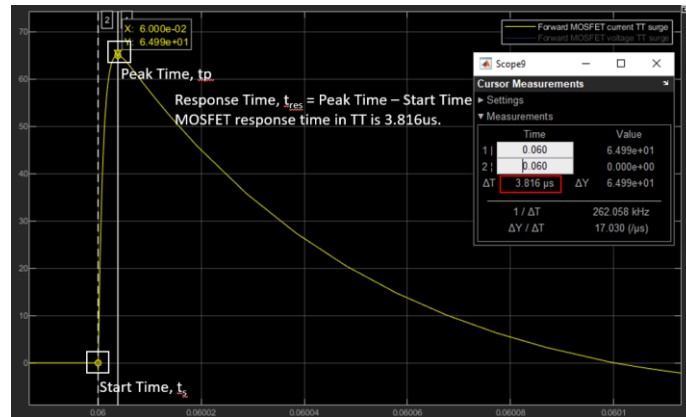


Figure 4.29: Measurement of the response time of forward MOSFET in TT earthing system

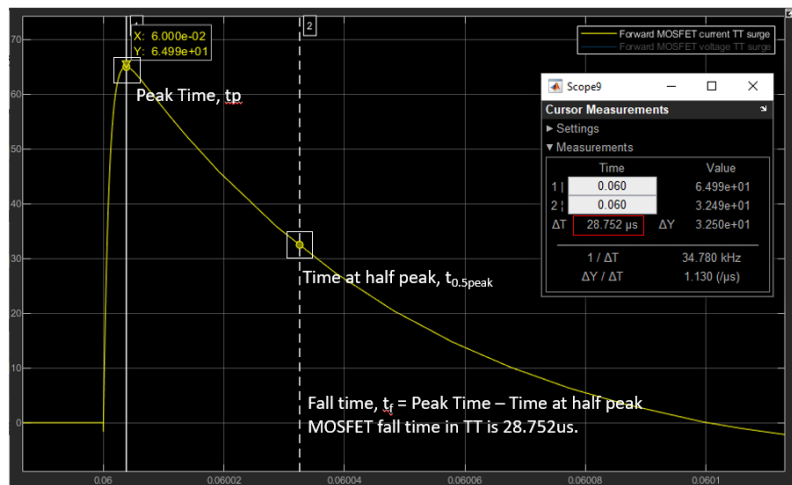


Figure 4.30: Measurement of the fall time of forward MOSFET in TT earthing system

Using the same method applied in measuring the response time and fall time of the MOV, the response time of the forward MOSFET is found to be 3.816 μs . At the same time, the fall time of the forward MOSFET is 28.752 μs . Figure 4.29 and 4.30 shows the measuring result for the response time and fall time of the MOV.

4.5.3 Impact of grounding resistance value on MOSFET performance

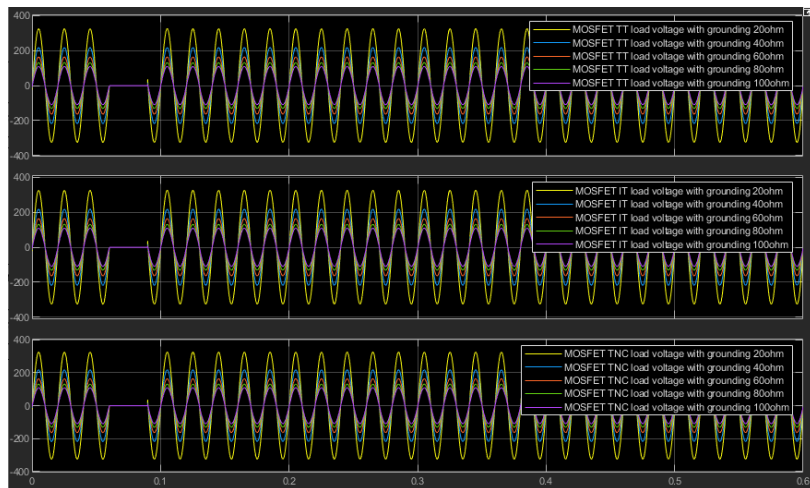


Figure 4.31: Load voltage waveform with MOSFET when grounding resistance increases

To study the impact of grounding resistance value on the MOSFET performance, the grounding resistance in all earthing systems increases from $20\ \Omega$ to $100\ \Omega$. As shown in Figure 4.31, the voltage waveform across the AC load in all earthing systems is the same when the grounding resistance increases. The voltage waveform peak value reduces as the grounding resistance increases. This is due to the series connection between the $20\ \Omega$ load and the grounding in the network. The grounding absorbs more voltage as the grounding resistance is more excellent than the $20\ \Omega$ load.

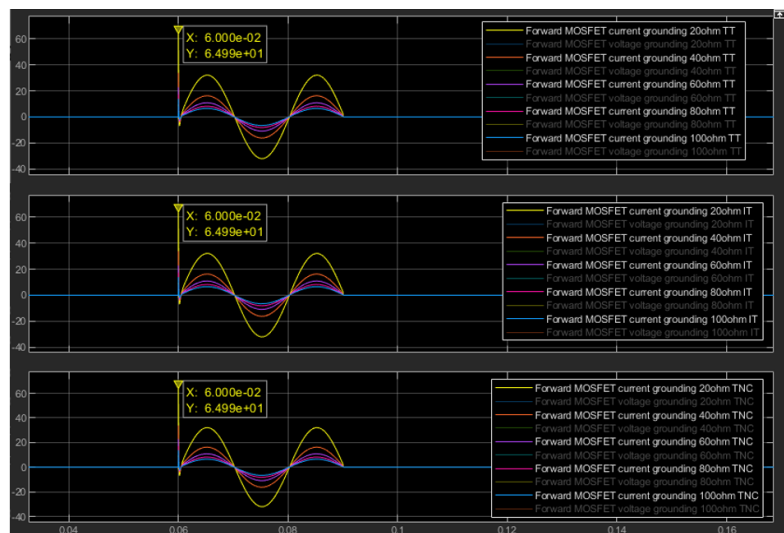


Figure 4.32: Operating current waveform of forward MOSFET when grounding resistance increases

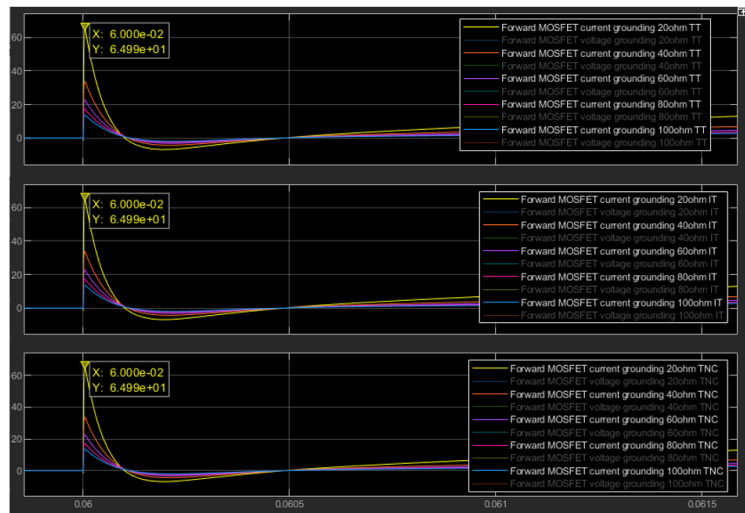


Figure 4.33: Surge current waveform of forward MOSFET when grounding resistance increases

For the spike waveform and current waveform and across the forward MOSFET, the peak value and the waveform reduce when the grounding resistance increases. This relationship is depicted in Figure 4.32 and Figure 4.33. Based on both figures, the current waveform and the spike waveform in all earthing systems are similar. These results imply that the MOSFET performance is only impacted by the increase of the grounding resistance and not by the earthing system types. Since the changes made by increasing grounding resistance at all earthing systems are the same, the spike waveform at the TT earthing system will only be observed.

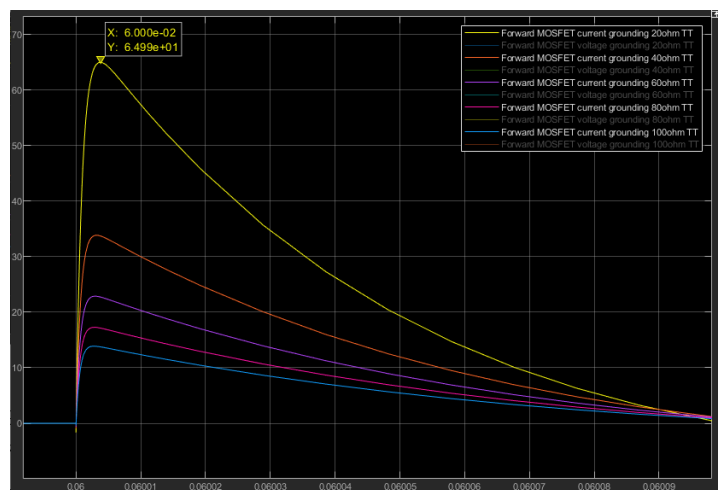


Figure 4.34: Surge current waveform of forward MOSFET when grounding resistance increases in TT earthing system

Table 4.5: Summary of the MOSFET protection parameter in different grounding resistance

Grounding Resistance (Ω)	Surge current of forward MOSFET (A)	Response Time, t_{res} (μs)	Fall Time, t_{fall} (μs)
20	64.99	3.816	28.752
40	33.69	3.110	33.273
60	22.78	2.803	34.816
80	17.21	2.748	35.705
100	13.83	2.653	36.785

Figure 4.34 shows the spike waveform across the MOSFET when the grounding resistance increases in an enlarged view. Based on Table 4.5, the MOSFET clamps off a lesser current when the grounding resistance increases. This is because the switching on of the MOSFET during a surge event creates a short circuit path to the grounding. The MOSFET is connected in common mode and parallel against the 20Ω load. The current will not flow towards the 20Ω load but the grounding. As the grounding resistance value increases, the MOSFET will divert lesser current to the ground because the high resistance prevents more current from flowing through. Besides, this explanation is also verified by using Ohms Law, $V = IR$. When the resistance increases, the current will decrease. The decrease in the MOSFET clamping performance is acceptable, and a lower grounding resistance is more suitable for the MOSFET.

Furthermore, the forward MOSFET response time decreases when the grounding resistance value increases. This result means that the forward MOSFET allows surge current to flow quicker towards the grounding with high resistance. This is agreed because the amount of current flowing through the MOSFET is less due to the high grounding resistance. As such, a high grounding resistance shortens the forward MOSFET response time.

On the other hand, the fall time of the forward MOSFET increases together with the grounding resistance. This relationship implies that the increase in grounding resistance slows down the forward MOSFET's ability to clear off the surge current. Although the surge current clamped by the forward

MOSFET is significantly less, the high grounding resistance still slows down the clamped surge in passing through the grounding to reach the earth.

In short, the MOSFET is more suitable for operating with low grounding resistivity. This is because the forward MOSFET needs to clamp off more surge current during the surge event. Besides, by comparing the response time and the fall time, the time difference of the fall time between the lowest and highest grounding resistance is 8.033 μs . At the same time, the time difference for the response time is only 1.153 μs .

4.6 Comparison between MOSFET and MOV performance

Table 4.6: Comparison between the response time and fall time of the forward MOSFET and the MOV

Grounding Resistance (Ω)	Response Time, t_{res} (μs)		Fall Time, t_{fall} (μs)	
	MOV	Forward MOSFET	MOV	Forward MOSFET
20	3.843	3.816	48.463	28.752
40	3.016	3.110	37.045	33.273
60	2.740	2.803	36.051	34.816
80	2.664	2.748	35.033	35.705
100	2.650	2.653	34.897	36.785

Table 4.6 compares the response time and fall time of the forward MOSFET and the MOV. For the response time, both SPD's response time gets faster when the grounding resistance increases. The response time for both SPDs is close to each other. Although the forward MOSFET responds faster than the MOV at low grounding resistance, the MOV gets a faster response when the grounding resistance increases. Similarly, this relationship also occurs when both SPDs are compared for the fall time. Unlike the conventional SPD, the MOSFET, which belongs to a power electronic type SPD, is a fast-switching device that activates fast and recovers back to normal operating mode fast.

This result concludes that the forward MOSFET is more suitable for the earthing system with grounding resistance lower than 20 Ω . In comparison, the MOV is suitable for the earthing system with high grounding resistance.

4.7 Harmonic distortion

This section discusses the impact of harmonic distortion on the SPD performance during a surge event. Firstly, the load voltage waveform when harmonic distortion is applied with and without surge for all earthing system are discussed. Secondly, the clamping performance and protection efficiency of the MOV and MOSFET with and without harmonics. Lastly, the impact of grounding resistance on the MOSFET and MOV in the situation between normal operating conditions and harmonic distortion environment are compared.

4.7.1 Different earthing system with harmonic distortion applied

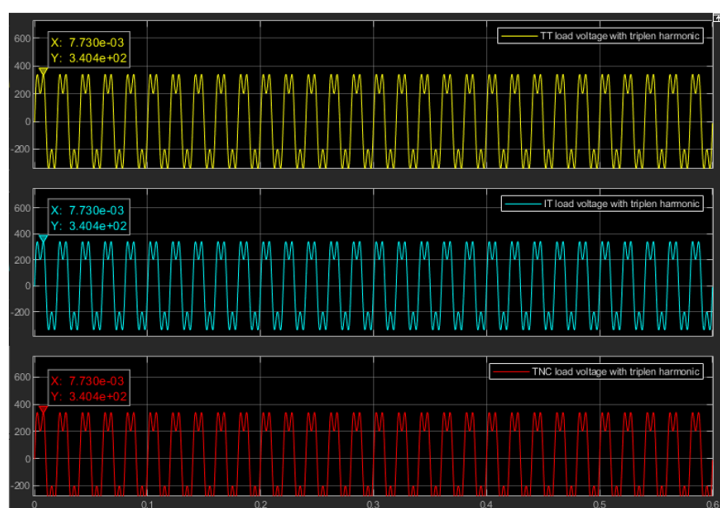


Figure 4.35: Load voltage waveform with triplen harmonic in different earthing system

In this project, the harmonic distortion applied is the triplen harmonics. Based on Figure 4.35, all three earthing systems have the same load voltage waveform and peak voltage value. The 240 Vrms load is still supplied in all three earthing systems with a peak voltage of 340.4 V. However, the waveform supplied to the load is not a perfect AC sinusoidal wave due to the distortion caused by the triplen harmonics. This result is desired as the triplen harmonic occurrence will affect the supplying voltage to any load connected to the earthing system.

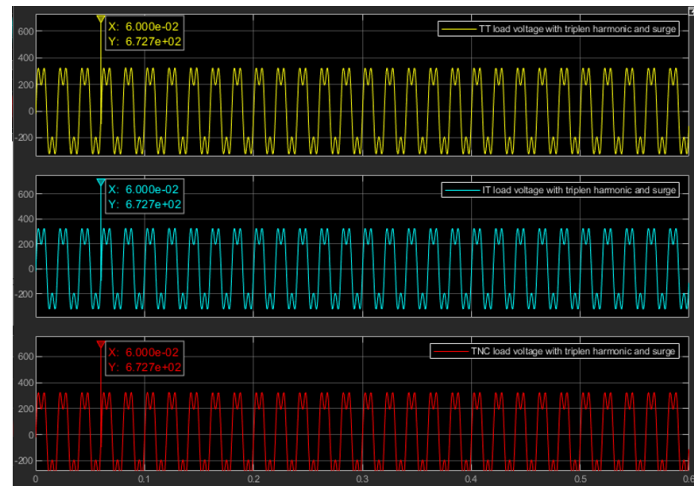


Figure 4.36: Load voltage waveform with triplen harmonic and surge in different earthing system

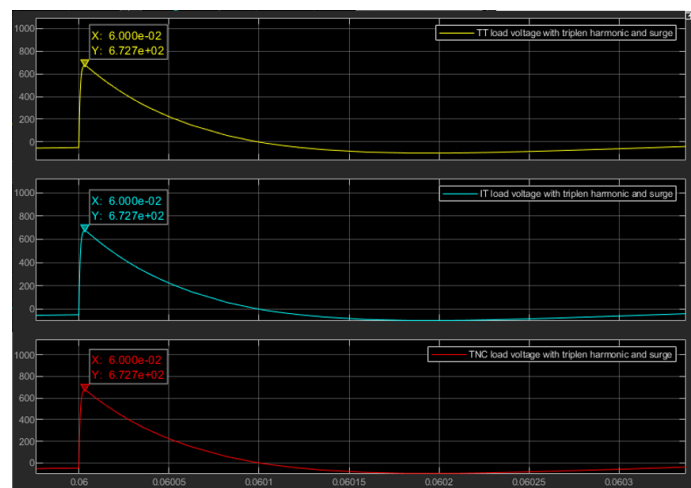


Figure 4.37: Overvoltage surge waveform with triplen harmonic different earthing system

From Figure 4.36, when the surge is applied for 0.06 seconds, the surge voltage peak value in their earthing system is the same at 672.7 V. Besides, in Figure 4.37, the surge voltage waveform in all three earthing systems is similar. This result is acceptable, implying that the occurrence of harmonic distortion across the earthing system does not affect the purely generated surge waveform.

4.7.2 Effect of harmonic distortion on the MOV performance

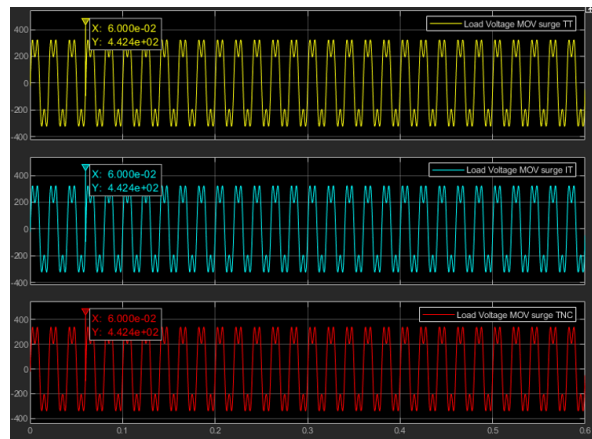


Figure 4.38: Load voltage waveform with surge, harmonic and MOV applied in different earthing systems

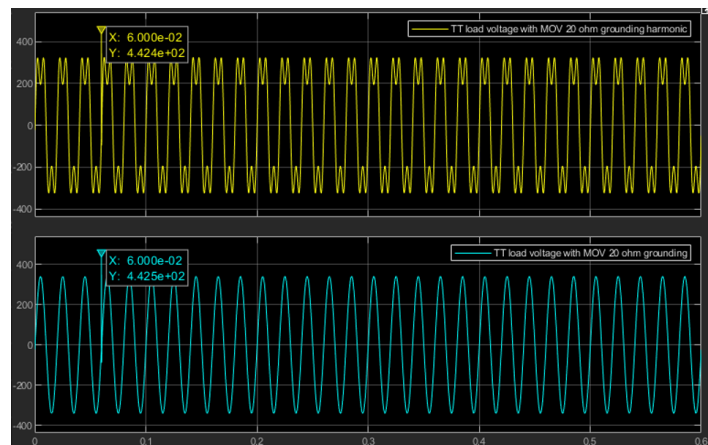


Figure 4.39: Load voltage waveform with and without harmonic at MOV TT earthing system

Based on Figure 4.38, the peak clamping voltage value of the MOV in all earthing systems is similar at 442.4 V. Since there is no difference between the earthing system when the triplen harmonic is added, this section will only study the effect of the triplen harmonic on the MOV performance for the TT earthing system. As shown in Figure 4.39, the clamping performance of the MOV at the triplen harmonic distorted earthing system is almost similar to the earthing system operated under normal conditions. The distorted MOV clamps off 0.1 V more than the normal operated MOV. This result implies that the harmonic distortion does not reduce but improves the MOV clamping performance.

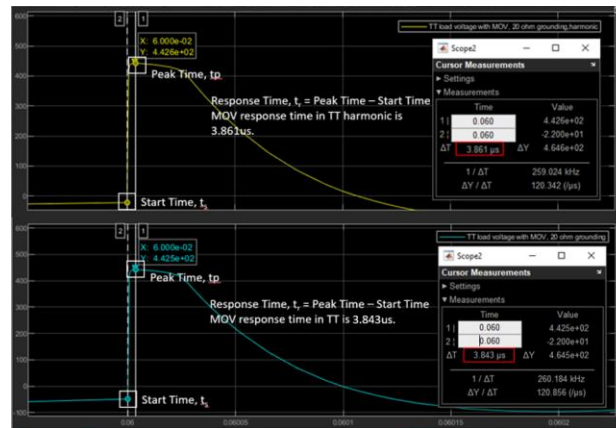


Figure 4.40: Measurement of MOV response time with and without harmonic

As shown in Figure 4.40, the MOV clamped surge waveform at the typical operating earthing system and triplen harmonic distorted earthing systems are the same. This shows that the harmonic distortion does not affect the clamping performance of the MOV too. By measuring the response time, the distorted MOV with $3.861 \mu\text{s}$ is slower than the normal operated MOV with $3.843 \mu\text{s}$. This result is expected as the voltage supplied to the MOV is distorted by the triplen harmonic, slowing down the MOV in reducing the internal resistance from high to low for diverting the surge to the ground.

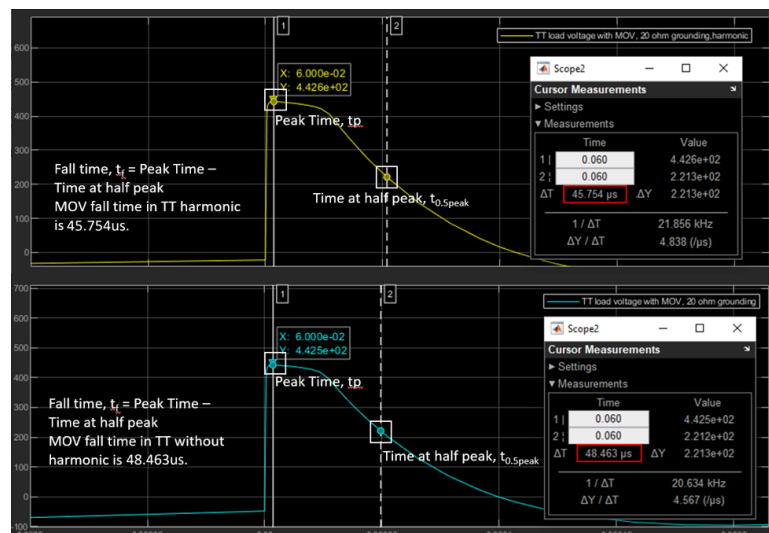


Figure 4.41: Measurement of MOV fall time with and without harmonic

As shown in Figure 4.41, the fall time of the harmonic distorted MOV with $45.754 \mu\text{s}$ is faster than the normal operated MOV by $2.709 \mu\text{s}$. This result implies that the existence of a triplen harmonic does not affect the internal

resistance of the MOV from rising back to a high level after diverting the clamped surge. Thus, the MOV response time will only be delayed by the existence of the harmonic distortion, whereas the fall time is not affected.

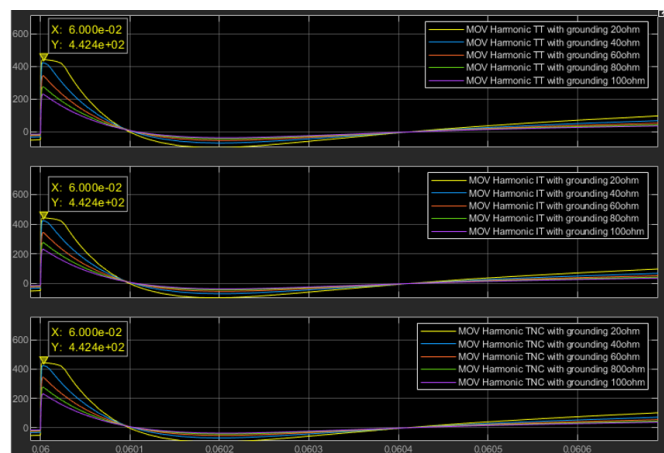


Figure 4.42: MOV clamped waveform at different earthing systems and grounding resistance with harmonic

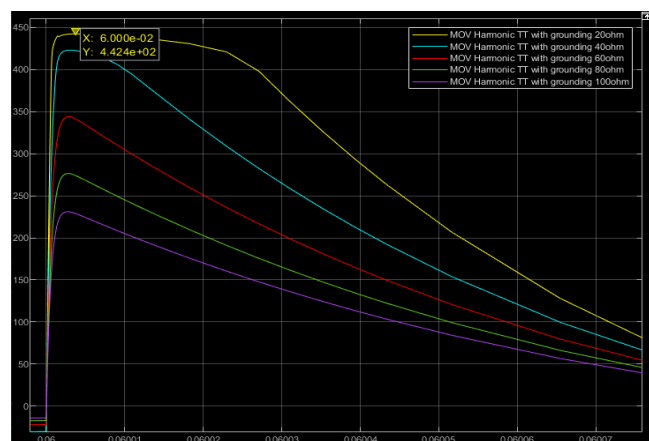


Figure 4.43: MOV clamped waveform at TT earthing systems and different grounding resistance with harmonic

As shown in Figure 4.42, when the grounding resistance increases, the MOV clamped surge voltage waveform in all earthing systems is the same. From Figure 4.43 and Table 4.7, the impact of the increasing grounding resistance on the MOV performance when operating in a triplen harmonic condition is similar to normal operating conditions. The peak clamping voltage of the distorted MOV decreases as the grounding resistance increases. Next, the

response time and fall time of the MOV under the triplen harmonic condition also decrease similarly to the normal operating condition.

Table 4.7: Comparison of the MOV protection parameter between harmonic and normal condition

Grounding Resistance (Ω)	Peak clamping voltage of MOV (V)		Response Time, t_r (μ s)		Fall Time, t_f (μ s)	
	Without harmonic	With harmonic	Without harmonic	With harmonic	Without harmonic	With harmonic
20	442.5	442.4	3.843	3.861	48.463	45.754
40	423.5	423.0	3.016	2.856	37.045	36.774
60	345.5	344.1	2.740	2.771	36.051	34.750
80	277.6	276.5	2.664	2.749	35.033	33.810
100	232.0	231.1	2.650	2.735	34.897	33.325

However, under triplen harmonic conditions, the MOV clamps more voltage than the normal operating condition MOV. Besides, the response time and fall time of the MOV are slower under the triplen harmonic condition. These results further justify that the existence of triplen harmonic the protection efficiency. This is because the triplen harmonic distorts the supplying voltage to the MOV, causing the MOV to reduce and recover the internal resistance slower. This causes the MOV to clamp away the surge voltage from the protected load and returns to normal operating condition slower. Thus, the existence of harmonic distortion weakens the slows down the response time and fall time of a MOV.

4.7.3 Effect of harmonic distortion on the MOSFET performance

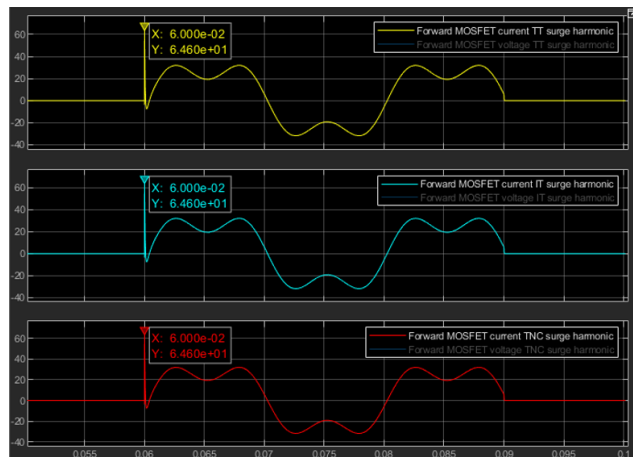


Figure 4.44: Forward MOSFET surge operating current waveform at different earthing system with harmonic applied

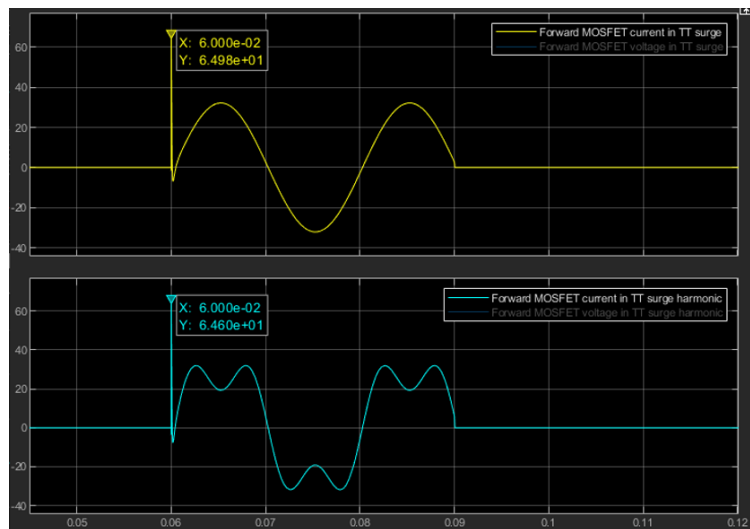


Figure 4.45: Forward MOSFET surge operating current waveform at TT earthing system with and without harmonic applied

Based on Figure 4.44, the spike peak value of the forward MOSFET in all earthing systems with triplen harmonic are similar at 64.6 A. Since there is no difference between the earthing system when the triplen harmonic is added, this section will only study the effect of the triplen harmonic on the forward MOSFET performance for the TT earthing system. As shown in Figure 4.45, the forward MOSFET with triplen harmonic clamps off 3.8 A lesser than the normal operating condition is performing weaker. This result implies that the harmonic distortion weakens the forward MOSFET clamping performance.

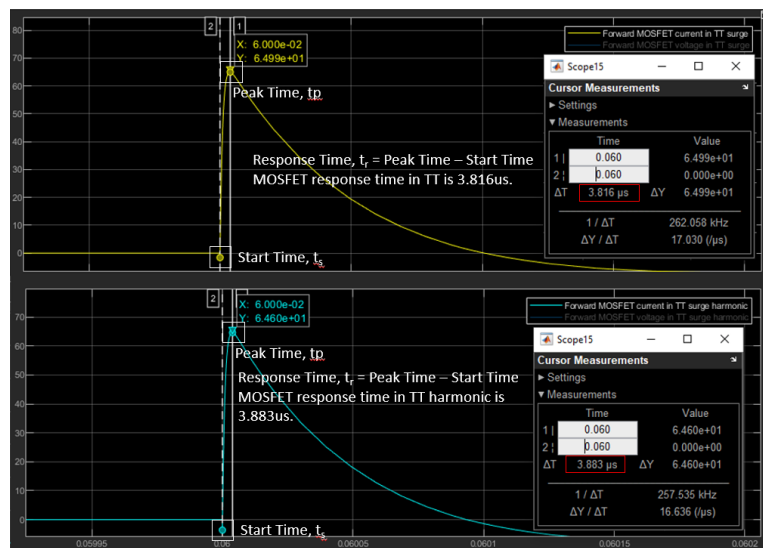


Figure 4.46: Measurement of Forward MOSFET response time with and without harmonic applied

As shown in Figure 4.46, the forward MOSFET spike waveform at the normal operating and triplen harmonic conditions are the same. By measuring the response time, the forward MOSFET under the triplen harmonic condition is slower than the normal operating condition by 0.067 μ s. This result is expected as the voltage supplied to the forward MOSFET is distorted by the triplen harmonic, delaying the forward MOSFET switch on speed. As such, the forward MOSFET delays creating the short-circuit path for diverting the surge to the ground.

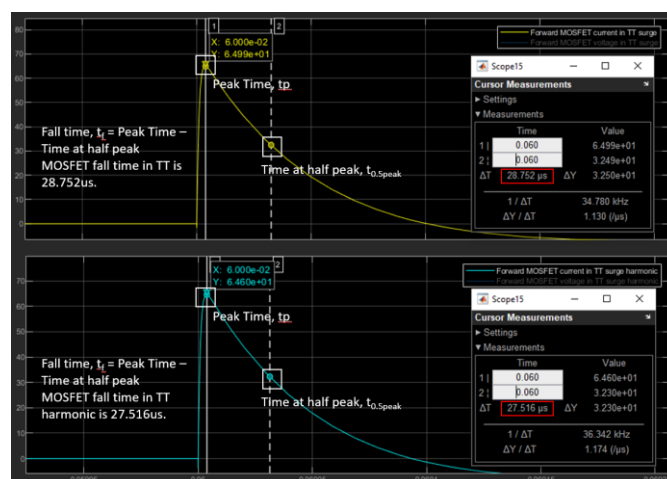


Figure 4.47: Measurement of Forward MOSFET fall time with and without harmonic applied

As shown in Figure 4.47, the fall time of the forward MOSFET operating under triplen harmonic condition is faster than the normal operating condition by $1.236 \mu\text{s}$. This result implies that the existence of a triplen harmonic does not delay the forward MOSFET from returning to normal operating conditions. Thus, the harmonic distortion will only delay the forward MOSFET response time, whereas the fall time is not affected.

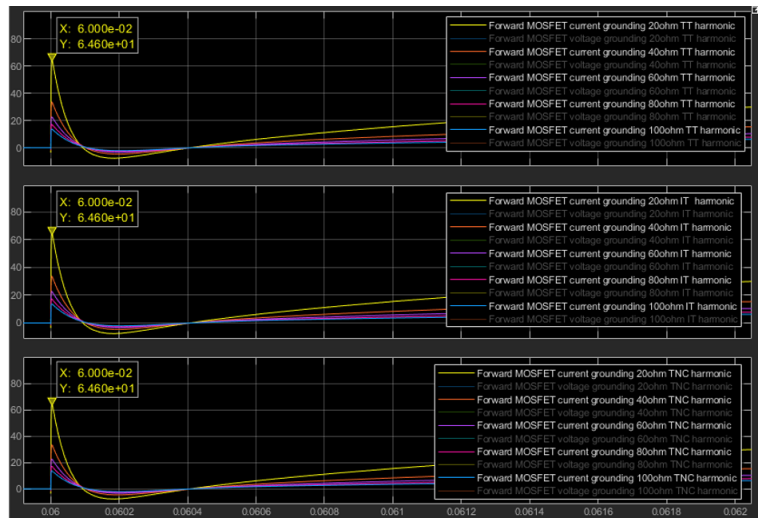


Figure 4.48: Forward MOSFET surge current waveform at different earthing systems and grounding resistance with harmonic

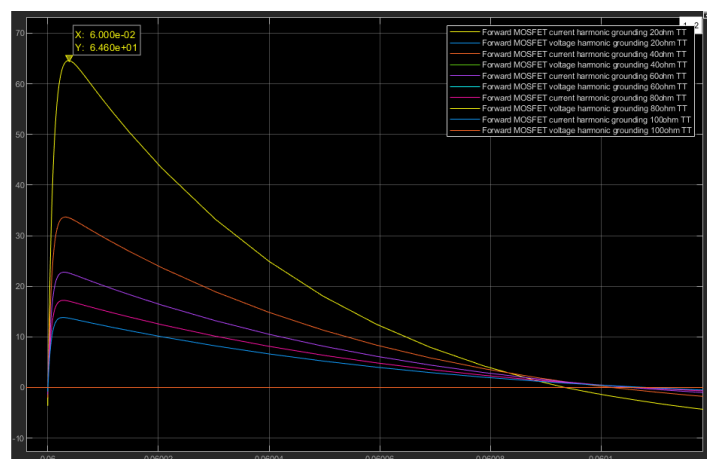


Figure 4.49: Forward MOSFET surge current waveform at TT earthing systems and different grounding resistance with harmonic

As shown in Figure 4.48, when the grounding resistance increases, the forward MOSFET spike waveform in all earthing systems is the same. From

Figure 4.49 and Table 4.8, the increasing grounding resistance on the forward MOSFET performance when operating under the triplen harmonic condition is similar to the normal operating condition. The forward MOSFET under both conditions clamps off lesser surge current as of the grounding resistance increases. Next, the forward MOSFET's response time and fall time under both conditions also decrease similarly.

Table 4.8: Comparison of the forward MOSFET protection parameter between harmonic and normal condition

Grounding Resistance (Ω)	Surge current of F. MOSFET (A)		Response Time, t_{res}		Fall Time, t_{fall} (μs)	
	Without harmonic	With harmonic	Without harmonic	With harmonic	Without harmonic	With harmonic
20	64.99	64.60	3.816	3.883	28.752	27.516
40	33.85	33.69	3.110	3.150	33.273	32.076
60	22.88	22.78	2.803	2.870	34.816	33.639
80	17.28	17.21	2.748	2.830	35.705	33.582
100	13.88	13.83	2.653	2.790	36.785	35.164

However, under triplen harmonic conditions, the forward MOSFET clamps a lesser current than the normal operating condition. Besides, the response time of the triplen harmonic condition is slower. At the same time, the fall time under triplen harmonic condition is faster than the normal operating condition. These results further justify that triplen harmonics weaken the forward MOSFET clamping performance and protection efficiency. The triplen harmonic distorts the voltage supplied to the forward MOSFET, causing a delay in switching on the forward MOSFET and creating the short circuit path to the ground. Thus, similar to the MOV, the existence of harmonic distortion weakens the clamping performance and slows down the response time of the forward MOSFET. In conclusion, the forward MOSFET and MOV are affected by triplen harmonics.

CHAPTER 5

CONCLUSIONS AND RECOMMENDATIONS

5.1 Conclusions

This project investigates the effect of different grounding layouts on SPD's protection efficiency. By founding out that power surges can happen either externally or internally in a system. This surge generator circuit imitated the lightning strike waveform of 1.2/50 μ s and was designed according to the IEC 61000-4-5. This surge generator was used as a source of surge to induce into the earthing systems, created via the MATLAB Simulink software. The earthing systems of TT, IT, and TNC are also created according to their earthing circuit characteristics. The MOV and MOSFET are connected to these earthing systems as the SPD. Both SPDs are tested with different grounding resistance and triplen harmonics.

This project proves that each SPD's performance and protection efficiency are not affected by the difference in the earthing system layout. Besides, the project found out that varying the grounding resistance impacts both SPDs differently. MOSFET provides fast response time and diverts more surge current under low grounding resistance condition. High grounding resistance is suitable for the MOV as this improves the clamping performance, response time, and fall time. Lastly, this project verifies that the existence of harmonic distortion such as the triplen harmonic impacts the overall performance for both of the SPDs. Due to the distorted voltage supplied, the clamping performance for both SPDs is weakened. Furthermore, the response time for both of the SPDs is also delayed.

In conclusion, the difference in the earthing system layout does not affect the performance of an SPD. Besides, the MOV is suitable for low grounding resistance conditions, and the MOSFET is suitable for high grounding resistance conditions. However, the earthing system with low grounding resistance is more desirable as these eases the diverting of surge current to the ground. Lastly, SPD must avoid harmonic distortion as this will weaken their performance.

5.2 Recommendations for future work

Since the MOSFET is a new type of power device SPD, more research and experiment under different conditions and scenarios must be conducted to verify its surge protection performance. Besides, a physical experiment must be carried out to verify further the protection performance of the MOV and MOSFET in different earthing layouts and different grounding resistance. This is because environmental factors such as the soil mineral content, moisture content, and soil resistivity might affect the MOSFET and MOV surge protection performance.

REFERENCES

- Lightning & Surge Protection. (2021). [online]. Available at: <https://www.m-system.co.jp/mssenglish/service/emmrester.pdf>.
- Science Learning Hub. (2014). *Lightning explained*. [online] Available at: <https://www.sciencelearn.org.nz/resources/239-lightning-explained>.
- Keeton, G. (n.d.). *How To Prevent an Inductive Load from Damaging Your Power Supply*. [online] blog.powerandtest.com. Available at: <http://blog.powerandtest.com/blog/prevent-an-inductive-load-from-damaging-your-power-supply>
- Waluyo, W., Syahrial, S., Nugraha, S. and Permana JR, Y. (2016). Prototype Design and Analysis of Miniature Pulse Discharge Current Generator on Various Burdens. *International Journal on Electrical Engineering and Informatics*, 8(3), pp.472–493.
- Portal, E.-E.E. (2016). *Best practice for using surge protective devices (SPDs) and RCDs together*. [online] EEP - Electrical Engineering Portal. Available at: <https://electrical-engineering-portal.com/surge-protective-devices-spds-red>
- Mitolo, M., Sutherland, P.E. and Natarajan, R. (2010). Effects of High Fault Currents on Ground Grid Design. *IEEE Transactions on Industry Applications*, 46(3), pp.1118–1124.
- Kazmi, D., Qasim, S., Fahad, I., Siddiqui and Azhar, S. (2016). *Exploring the Relationship between Moisture Content and Electrical Resistivity for Sandy and Silty Soils*. [online], pp.42–47. Available at: [http://www.ijesi.org/papers/Vol\(5\)7/F0507042047.pdf](http://www.ijesi.org/papers/Vol(5)7/F0507042047.pdf)
- Mari, L. (2020). *An Introduction to Soil Resistivity - Technical Articles*. [online] Available at: <https://eepower.com/technical-articles/an-introduction-to-soil-resistivity/#>.
- LIGHTNING PROTECTION GUIDE 3rd updated Edition. (2015). [online]. Available at: <https://www.dehn-international.com/sites/default/files/media/files/lpg-2015-e-complete.pdf>.

Electrical Notes & Articles. (2020). *Methods of Earth Resistance Testing (Part-1)*. [online] Available at:
<https://electricalnotes.wordpress.com/2020/02/12/methods-of-earth-resistance-testing-part-1/>

Carobbi, C.F.M. and Bonci, A. (2013). Elementary and ideal equivalent circuit model of the 1, 2/50-8/20 μ s combination wave generator. *IEEE Electromagnetic Compatibility Magazine*, 2(4), pp.51–57.

Trotsenko, Y., Brzhezitsky, V., Protsenko, O. and Haran, Y., 2021. Simulation of impulse current generator for testing surge arresters using frequency-dependent models. *Technology audit and production reserves*, 1(1(57)), pp.25-29.

electrical.theiet.org. (n.d.). *Inspection and testing of earth electrodes*. [online] Available at: <https://electrical.theiet.org/wiring-matters/years/2017/65-may-2017/inspection-and-testing-of-earth-electrodes/>.

Portal, E.-E.E. (2016). *3 good ways to improve earth electrode resistance / EEP*. [online] EEP - Electrical Engineering Portal. Available at:
<https://electrical-engineering-portal.com/improve-earth-electrode-resistance>.

Nemasurge.org. (2019). *How SPDs work / NEMA Surge protection Institute*. [online] Available at: <https://www.nemasurge.org/how-spd-s-work/>.

Gomes, C. (2011). On the selection and installation of surge protection devices in a TT wiring system for equipment and human safety. *Safety Science*, 49(6), pp.861–870.

Melo, L.B.B. de, Silva, B.M., Peixoto, D.S., Chiarini, T.P.A., de Oliveira, G.C. and Curi, N. (2021). Effect of compaction on the relationship between electrical resistivity and soil water content in Oxisol. *Soil and Tillage Research*, 208, p.104876.

Androvitsaneas, V.P., Damianaki, K.D., Christodoulou, C.A. and Gonos, I.F. (2020). Effect of Soil Resistivity Measurement on the Safe Design of Grounding Systems. *Energies*, 13(12), p.3170.

APPENDICES

Appendix A: IEC 61000-4-5 STANDARD

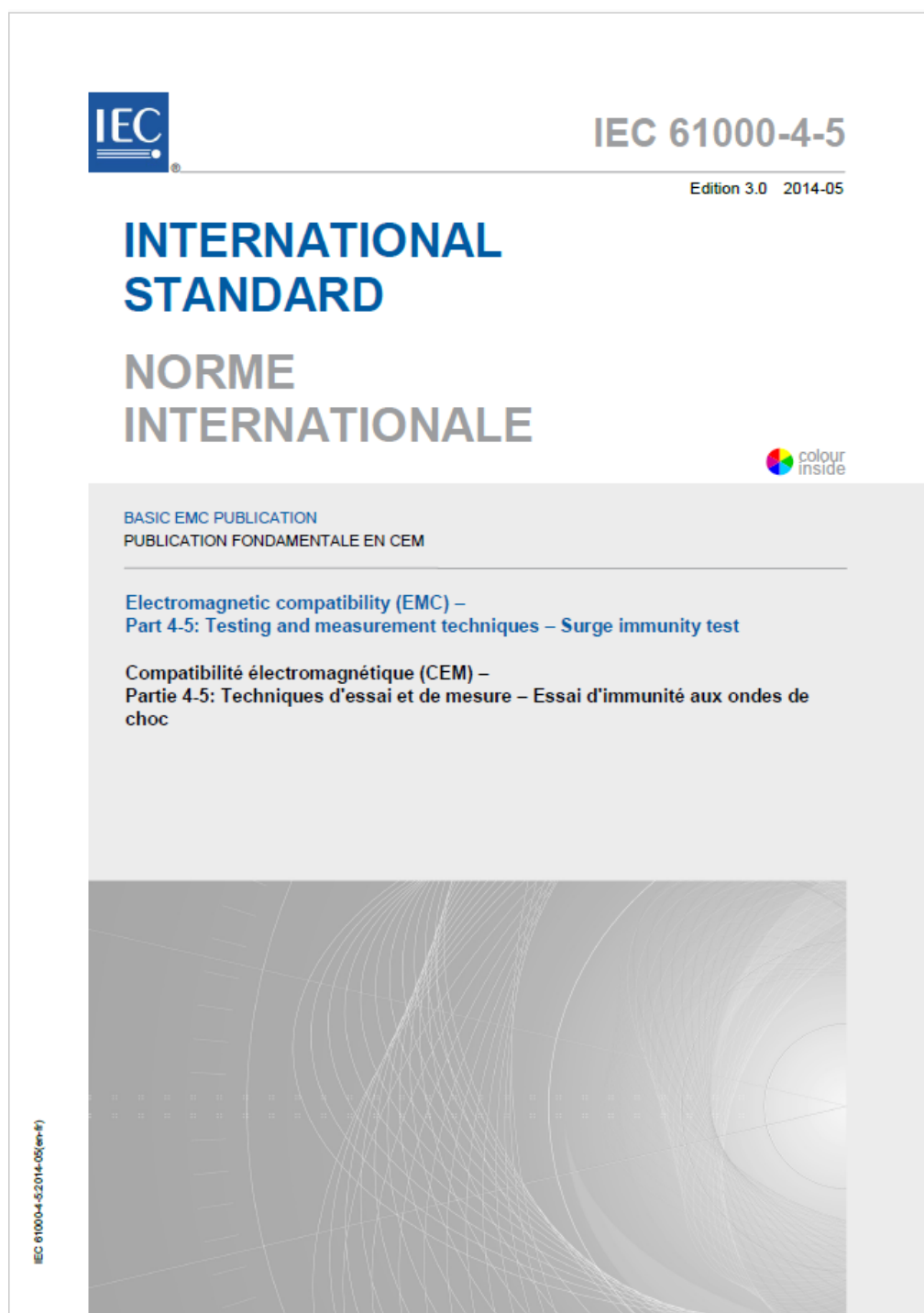


Table 1 – Test levels

Level	Open-circuit test voltage	
	kV	
	Line-to-line	Line-to-ground ^b
1	---	0,5
2	0,5	1
3	1	2
4	2	4
X ^a	Special	Special

^a "X" can be any level, above, below or in between the others. The level shall be specified in the dedicated equipment specification.

^b For symmetrical interconnection lines the test can be applied to multiple lines simultaneously with respect to ground, i.e. "lines to ground".

The test levels shall be selected according to the installation conditions; classes of installation are given in Annex C.

The test shall be applied at all test levels in Table 1 up to and including the specified test level (see 8.3).

For selection of the test levels for the different interfaces, refer to Annex B.

6 Test instrumentation

6.1 General

Two types of combination wave generators are specified. Each has its own particular applications, depending on the type of port to be tested. The 10/700 μ s combination wave generator is used to test ports intended for connection to outdoor symmetrical communication lines (see Annex A). The 1,2/50 μ s combination wave generator is used in all other cases.

6.2 1,2/50 μ s combination wave generator

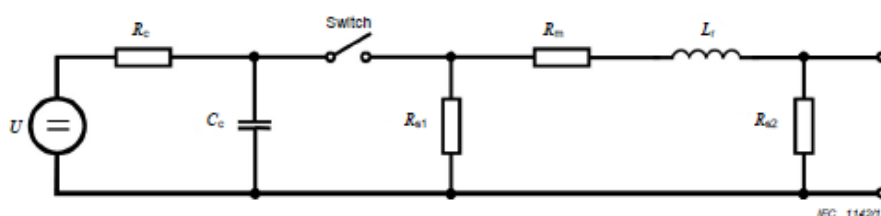
6.2.1 General

It is the intention of this standard that the output waveforms meet specifications at the point where they are to be applied to the EUT. Waveforms are specified as open-circuit voltage and short-circuit current and therefore shall be measured without the EUT connected. In the case of an a.c. or d.c. powered product where the surge is applied to the a.c. or d.c. supply lines, the output waveforms shall be as specified in Tables 4, 5, and 6. In the case where the surge is applied directly from the generator output terminals, the waveforms shall be as specified in Table 2. It is not intended that the waveforms meet specifications both at the generator output and at the output of coupling/decoupling networks simultaneously, but only as applied to the EUT.

This generator is intended to generate a surge having:

- an open-circuit voltage front time of 1,2 μ s;
- an open-circuit voltage duration of 50 μ s;
- a short-circuit current front time of 8 μ s;
- a short-circuit current duration of 20 μ s.

A simplified circuit diagram of the generator is given in Figure 1. The values for the different components R_{S1} , R_{S2} , R_M , L_T , and C_C are selected so that the generator delivers a 1,2/50 μ s voltage surge at open-circuit conditions and an 8/20 μ s current surge into a short-circuit.



Key

U	High-voltage source
R_c	Charging resistor
C_c	Energy storage capacitor
R_s	Impulse duration shaping resistors
R_M	Impedance matching resistor
L_T	Rise time shaping inductor

Figure 1 – Simplified circuit diagram of the combination wave generator

The ratio of peak open-circuit output voltage to peak short-circuit current at the same output port of a combination wave generator shall be considered as the effective output impedance. For this generator, the ratio defines an effective output impedance of 2 Ω .

When the generator output is connected to the EUT, the waveform of the voltage and current is a function of the EUT input impedance. This impedance may change during surges to equipment due either to proper operation of the installed protection devices, or to flash over or component breakdown if the protection devices are absent or inoperative. Therefore, the 1,2/50 μ s voltage and the 8/20 μ s current waves should be available from the same generator output as required by the load.

6.2.2 Performance characteristics of the generator

Polarity	positive and negative
Phase shifting	in a range between 0° to 360° relative to the phase angle of the a.c. line voltage to the EUT with a tolerance of $\pm 10^\circ$
Repetition rate	1 per minute or faster
Open-circuit peak output voltage	adjustable from 0,5 kV to the required test level
Waveform of the surge voltage	see Table 2 and Figure 2
Output voltage setting tolerance	see Table 3
Short-circuit peak output current	depends on peak voltage setting (see Tables 2 and 3)
Waveform of the surge current	see Table 2 and Figure 3

NOTE The time parameters are valid for the short-circuit current at the generator output without a 10 Ω resistor (see 6.3).

Short-circuit output current tolerance see Table 3

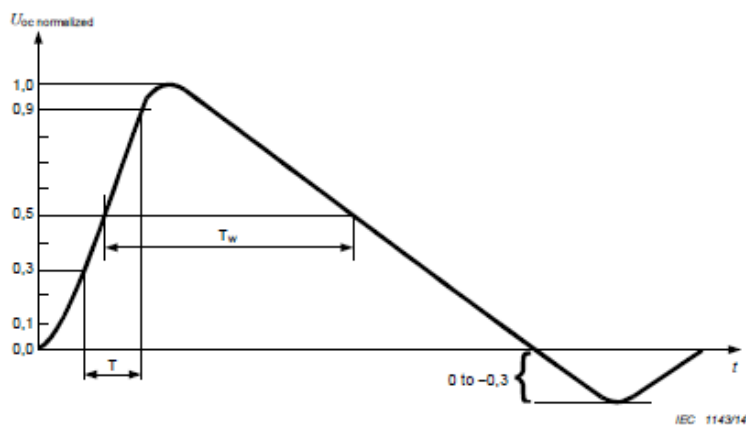
Table 2 – Definitions of the waveform parameters 1,2/50 μs and 8/20 μs

	Front time T_f μs	Duration T_d μs
Open-circuit voltage	$T_f = 1,67 \times T = 1,2 \pm 30 \%$	$T_d = T_w = 50 \pm 20 \%$
Short-circuit current	$T_f = 1,25 \times T_f = 8 \pm 20 \%$	$T_d = 1,18 \times T_w = 20 \pm 20 \%$

Table 3 – Relationship between peak open-circuit voltage and peak short-circuit current

Open-circuit peak voltage ± 10 % at generator output	Short-circuit peak current ± 10 % at generator output
0,5 kV	0,25 kA
1,0 kV	0,5 kA
2,0 kV	1,0 kA
4,0 kV	2,0 kA

A generator with floating output shall be used.

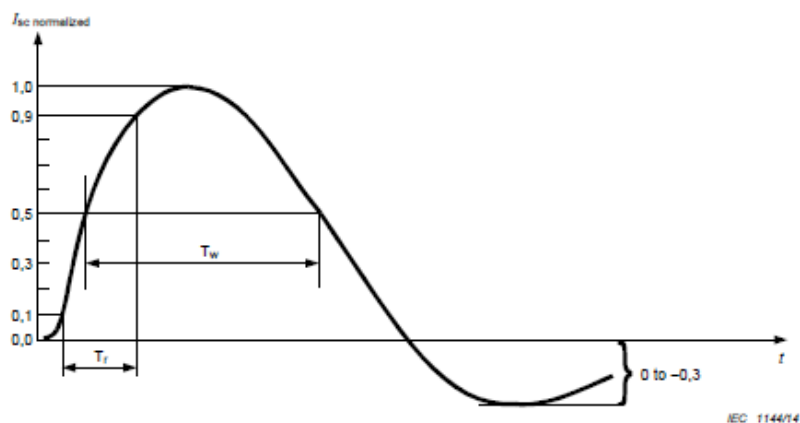


Front time: $T_f = 1,67 \times T = 1,2 \mu\text{s} \pm 30 \%$
Duration: $T_d = T_w = 50 \mu\text{s} \pm 20 \%$

NOTE The value 1,67 is the reciprocal of the difference between the 0,9 and 0,3 thresholds.

Figure 2 – Waveform of open-circuit voltage (1,2/50 μs) at the output of the generator with no CDN connected

The undershoot specification applies only at the generator output. At the output of the coupling/decoupling network there is no limitation on undershoot or overshoot.



Front time: $T_f = 1,25 \times T_f = 8 \mu\text{s} \pm 20 \%$
 Duration: $T_d = 1,18 \times T_w = 20 \mu\text{s} \pm 20 \%$

NOTE 1 The value 1,25 is the reciprocal of the difference between the 0,9 and 0,1 thresholds.

NOTE 2 The value 1,18 is derived from empirical data.

Figure 3 – Waveform of short-circuit current (8/20 μs) at the output of the generator with no CDN connected

The undershoot specification applies only at the generator output. At the output of the coupling/decoupling network there is no limitation on undershoot or overshoot.

6.2.3 Calibration of the generator

The test generator characteristics shall be calibrated in order to establish that they meet the requirements of this standard. For this purpose the following procedure shall be undertaken (see also Annex G).

The generator output shall be connected to a measuring system with a sufficient bandwidth, voltage and current capability to monitor the characteristics of the waveforms. Annex E provides information concerning the bandwidth of the surge waveforms.

If a current transformer (probe) is used to measure short-circuit current it should be selected so that saturation of the magnetic core does not take place. The lower (-3 dB) corner frequency of the probe should be less than 100 Hz.

The characteristics of the generator shall be measured through an external capacitor of 18 μF in series with the output, both under open-circuit (load greater than or equal to 10 k Ω) and short-circuit conditions at the same set voltage. If the 18 μF capacitor is implemented in the generator, no external 18 μF capacitor is required for calibration.

All performance characteristics stated in 6.2.2, with the exception of phase shifting, shall be met at the output of the generator. Phase shifting performance shall be met at the output of the CDN at 0°, 90°, 180° and 270° at one polarity.

NOTE When an additional internal or external resistor is added to the generator output to increase the effective source impedance from 2 Ω to e.g. 12 Ω or 42 Ω , according to the requirements of the test setup, the front time and the duration of test impulses at the output of the coupling network can be significantly changed.